nature portfolio

Peer Review File

Regulation of H+ transfer pathways promotes C-C coupling in acidic CO2 electroreduction

Corresponding Author: Professor Guoxiong Wang

This file contains all reviewer reports in order by version, followed by all author rebuttals in order by version.

Version 0:

Reviewer comments:

Reviewer #1

(Remarks to the Author)
This work reports a novel strategy to promote C–C coupling in CO2RR under acidic conditions by regulating the H^+ transfer pathway. The authors constructed a TCPP(M)-modified CuO nanosheet catalytic system and revealed the reaction mechanism combining in situ spectroscopy and DFT calculations. Focusing on the current hotspot and challenge of acidic CO2RR, this study presents clear scientific significance and potential application value. By integrating material design, in situ characterization, electrocatalytic performance testing, and theoretical calculations, the authors propose that organometallic porphyrin modification can regulate interfacial proton migration, thereby promoting *CO coupling to generate multi-carbon products. This concept is novel, and the overall results are convincing. Generally, this work has the potential for publication in Nature Communications; however, moderate revisions are required regarding the rigor of mechanistic demonstrations, the completeness of control experiments, and the clarity of data presentation.
MAJOR POINTS
1. Although the authors provided post-reaction ATR-FTIR and EDS mapping (Supplementary Figs. 16 and 18), these cannot completely rule out the demetallation of the porphyrin ring. High-resolution XPS of the post-reaction catalyst, especially the Co 2p and N 1s spectra, needs to be provided to confirm that the Co–N4 coordination structure remains intact after long-term electrolysis. In addition, ICP-MS testing should be performed on the post-reaction electrolyte to rule out Co leaching.
2. The control samples are insufficient, FE data for samples modified with only the organic molecules (without the metal center) should be added.
3. Although in situ EPR successfully captured the ·H signal, to prove that ·H is indeed directly involved in CO2 activation and hydrogenation (rather than in an unrelated, parallel side reaction), the authors should perform a radical quenching experiment. It is recommended to add a specific hydrogen radical scavenger (such as DMPO or other suitable trapping agents) to the electrolyte and observe whether the FE of C_{2+} drops significantly.
4. Regarding the use of PTFE instead of carbon paper in the stability tests, a specific and detailed implementation procedure should be provided in the Experimental section.
5. Comparative EPR analysis between TCo–CuO NS and bare CuO NS under a CO2 atmosphere is missing.
6. The current DFT analysis appears to focus primarily on energetics. To provide a deeper understanding of why H* readily spills over from the Co site, an electronic structure analysis is recommended. The authors should calculate and analyze the electron density of states, charge density difference, or Crystal Orbital Hamilton Population (COHP) for H-adsorption on the Co site. This could explain the thermodynamic and/or kinetic factors that favor the detachment of H* from the Co center.
MINOR POINTS
1. In Supplementary Fig. 33, the y-axis is labeled "Yield (mmol h-1 cm-2)". In chemistry, "Yield" is usually a percentage value; using "Production rate" or "Formation rate" would be scientifically more accurate.
2. In the main text, when mentioning that the Δv of the -COO stretching vibration "decreased from 209 cm^{-1} to 171 cm^{-1}", "Supplementary Fig. 16" should be directly cited in that specific sentence to ensure the clarity of the text.

Reviewer #2

(Remarks to the Author)
In this manuscript, Jin et al. presents a highly interesting and thoroughly investigated strategy to achieve efficient multicarbon (C2+) product generation in acidic CO2 electroreduction (CO2RR). By anchoring the molecular modifier TCPP(Co) onto CuO nanosheets, the authors constructed a dual-site synergistic interface. The manuscript convincingly demonstrates that TCPP(Co) can regulate the proton transfer pathway by promoting the formation of transient hydrogen

radicals and disrupting the interfacial water network, thereby facilitating asymmetric *CHO–*CO coupling on adjacent Cu sites while suppressing the competing hydrogen evolution reaction (HER). The catalyst achieved a highly competitive C2+ Faradaic efficiency of 89.5% at a high current density of 1 A cm^{-2} in a pH 2 electrolyte. Furthermore, the combination of in situ EPR, in situ SERS, AIMD, and static DFT provides multi-dimensional mechanistic insights. The manuscript is logically rigorous, and its results will be highly appealing to a broad readership in the fields of electrocatalysis and energy conversion. After the authors address the following minor concerns and clarify the related details, I believe this manuscript will fully meet the publication standards of Nature Communications. I recommend accepting it after minor revisions.

1. Quantitative analysis of catalyst loading. The authors mentioned concentration dependent performance (e.g., excessively coated TCo–CuO NS-3 led to decreased ECSA and performance due to the masking of active sites). However, absolute loading data for TCPP(Co) on the optimally performing TCo–CuO NS is not provided. It is recommended to provide data to precisely quantify the atomic ratio of Co/Cu.

2. Figure 3g demonstrates excellent 100-hour stability at 0.2 A/cm^2. Although the authors provided post-reaction characterizations (ATR-FTIR, TEM) after short-term testing, confirming the stability of the molecular modifier after the 100-hour test is crucial. It is recommended to perform post-reaction XPS and ATR-FTIR characterizations on the electrode after prolonged continuous electrolysis. This would strongly prove that the porphyrin macrocycle does not degrade or detach under prolonged cathodic polarization.

3. In the static DFT calculations (Figure 1), the authors use benzoic acid (BZA) to represent the TCPP(Co) modifier. While this is a reasonable simplification for studying the -COO-Cu electronic interaction, the BZA model lacks the bulky, hydrophobic porphyrin ring and the Co center. The authors should add a brief discussion or justification in the main text explaining why the BZA-Cu model is sufficient for describing the thermodynamics of C-C coupling. It should be explicitly stated that steric/hydrophobic effects and the Volmer step (H2O dissociation on Co) are considered in the AIMD and/or unit-cell DFT calculations that utilize the full TCPP(Co) model, respectively.

4. The manuscript elegantly proposes the generation of H-radicals on TCPP(Co) that participate in the hydrogenation of *CO to *CHO on copper. However, the physical pathway for this hydrogen transfer (the spillover effect) remains ambiguous. The authors should at minimum provide a thermodynamic discussion of the energy required for the H-species to migrate from the Co center (or the porphyrin's N atoms) to the adjacent copper surface or to directly attack the adsorbed *CO.

5. In the mechanism discussion section, the manuscript sometimes conflates experimental observations from in situ characterizations (e.g., SERS/EPR) with theoretical deductions from AIMD/DFT within the same sentence. This makes it difficult for readers to quickly distinguish between directly observed facts and model-based inferences. I recommend using clearer transitional phrases and introductory words to bridge sentences and paragraphs.

6. There are a few minor spelling and typographical errors in the manuscript, Main text, Line 213: The word "indentical" is misspelled and should be corrected to "identical". Main text, Line 491: There is a duplicated word in the phrase "with with experimentally"

Reviewer #3

(Remarks to the Author)
This manuscript presents a significant conceptual advance in acidic CO_2 electroreduction by introducing a strategy to regulate proton transfer rather than suppress it. The catalytic performance is outstanding and the integration of molecular and heterogeneous catalysis is highly promising.
However, the structural characterization does not yet fully support the proposed molecular–metal interface and dual-site mechanism. Strengthening the structural evidence would greatly enhance the rigor and impact of the work. I recommend minor revision.

1. The central premise of the manuscript relies on the formation of a well-defined molecular-metal interface, in which TCPP(Co) is anchored to the Cu surface via carboxylate coordination. However, the structural evience supporting this claim remains largely indirect. The authors rely on FT-IR shifts of -COO- group, XPS signals (Co 2p and N1s) , and HRTEM observations to support the anchoring of TCPP(Co). While these techniques confirm the presence of the molecular species, they do not provide definitive information regarding the binding configuration (monodentate or bidentate), the coordination geometry at the Cu surface or the orientation of the porphyrin relative to the catalyst. The authors should explain and show more direct evidence.

2. The manuscript claims uniform dispersion of TCPP(Co) based on EDS mapping; however, this technique lacks sufficient spatial resolution to assess molecular-scale distribution. Moreover, the manuscript does not provide quantitative information on the loading amount of TCPP(Co), surface coverage, or the density of active sites. This information is essential for understanding structure-activity relationships and for normalizing catalytic activity.
3. Structural stability of the molecular layer after long-term electrolysis should be more thoroughly characterized.

Version 1:

Reviewer comments:

Reviewer #1

(Remarks to the Author)
All concerns have been addressed, please accept this article.

Reviewer #2

(Remarks to the Author)
The revised manuscript can be now accepted for publication.

Reviewer #3

(Remarks to the Author)
The revised manuscript can be accepted.

Manuscript number: NCOMMS-26-011003

Title: Regulation of H^+ transfer pathways promotes C–C coupling in acidic CO_2 electroreduction

Response to Reviewer's comments

Dear Editor and Reviewers,

We would like to express our sincere gratitude to the editor and all reviewers for your time, professional evaluation, and constructive comments on our manuscript. We have carefully considered all the suggestions and have made comprehensive revisions to the manuscript accordingly. We believe that these revisions have significantly improved the rigor and clarity of our work. To facilitate your review process, we have provided a point-by-point response below. For clarity, the reviewers' original comments are shown in blue text, and the corresponding modifications made to the revised manuscript are highlighted in yellow. Please find our detailed responses as follows:

Reply to Reviewer #1:

This work reports a novel strategy to promote C–C coupling in CO_2RR under acidic conditions by regulating the H^+ transfer pathway. The authors constructed a TCPP(M)-modified CuO nanosheet catalytic system and revealed the reaction mechanism combining in situ spectroscopy and DFT calculations. Focusing on the current hotspot and challenge of acidic CO_2RR, this study presents clear scientific significance and potential application value. By integrating material design, in situ characterization, electrocatalytic performance testing, and theoretical calculations, the authors propose that organometallic porphyrin modification can regulate interfacial proton migration, thereby promoting *CO coupling to generate multi-carbon products. This concept is novel, and the overall results are convincing. Generally, this work has the potential for publication in *Nature Communications*; however, moderate revisions are required regarding the rigor of mechanistic demonstrations, the completeness of control experiments, and the clarity of data presentation.

Response: We would like to express our sincere gratitude to you for the highly positive evaluation and the thoughtful, constructive comments on our manuscript. We are greatly encouraged by your recognition of the scientific significance, novelty, and potential application value of our TCPP(M)-modified CuO nanosheet catalytic system for acidic CO_2RR. We also deeply appreciate your insightful suggestions regarding the rigor of our mechanistic demonstrations, the completeness of our control experiments, and the clarity of our data presentation. We completely agree that addressing these aspects is crucial for enhancing the quality and scientific rigor of this work. In accordance with your valuable advice, we have carefully made comprehensive revisions to the manuscript. We have conducted the necessary additional control experiments, strengthened our mechanistic discussions, and improved the clarity of the figures and data presentation. Please find our detailed point-by-point responses to your specific comments below.

1. Although the authors provided post-reaction ATR-FTIR and EDS mapping (Supplementary Figs. 16 and 18), these cannot completely rule out the demetallation of the porphyrin ring. High-resolution XPS of the post-reaction catalyst, especially the Co 2p and N 1s spectra, needs to be provided to confirm that the Co–N_4 coordination structure remains intact after long-term electrolysis. In addition, ICP-MS testing should be performed on the post-reaction electrolyte to rule out Co leaching.

Response: We sincerely thank the reviewer for pointing out this critical aspect. We agree that while attenuated total reflection Fourier transform infrared spectroscopy (ATR-FTIR) and energy dispersive X-ray spectroscopy (EDS) provide valuable information, high-resolution X-ray photoelectron spectroscopy (XPS) and inductively coupled plasma (ICP) analyses are indispensable for definitively ruling out the demetallation of the porphyrin ring and confirming the integrity of the active sites.

To address this, we have performed the requested experiments and updated the revised manuscript accordingly. To confirm the preservation of the local coordination environment, we conducted high-resolution XPS on the post-reaction catalyst following a 100 h continuous stability test at a current density of 0.2 A cm^{-2}. The

post-reaction Co 2p and N 1s spectra closely match those of the pristine catalyst. Specifically, the Co 2p spectra show no emergence of peaks corresponding to zero-valent metallic Co or CoO, and the N 1s spectra confirm the retention of the metal-nitrogen bonds (**Fig. R1**). This firmly demonstrates that the CoN_4 coordination structure remains structurally intact and highly stable without undergoing demetallation during long-term electrolysis.

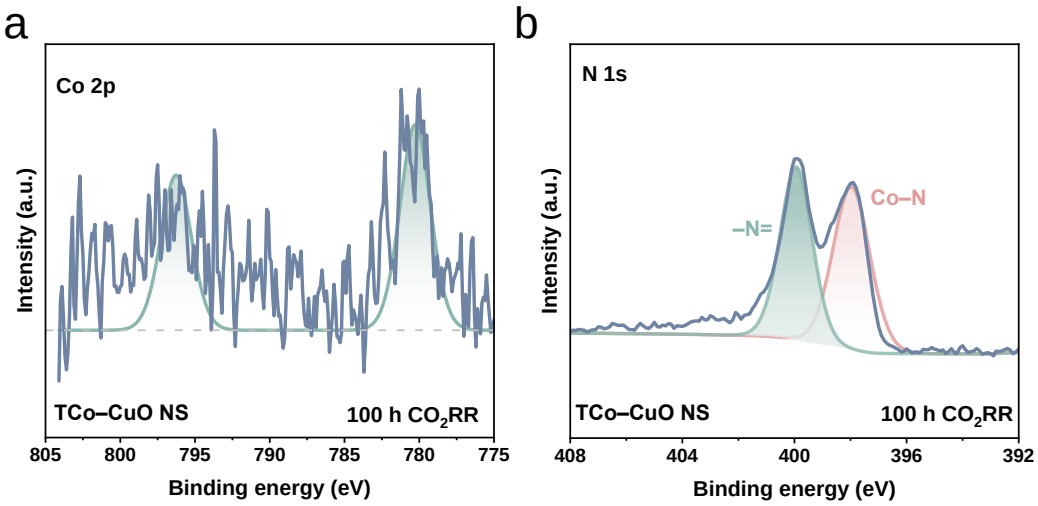

Fig. R1 | High-resolution XPS spectra of the catalyst after 100 h stability test at 0.2 A cm^{-2}, **a,** Co 2p and **b,** N 1s.

Furthermore, to explicitly address the concern regarding Co leaching into the solution, we dynamically monitored the 40 mL 1 M KCl pH 2 electrolyte by sampling it every hour during a 5 h continuous electrolysis test at the same working current density of 0.2 A cm^{-2}. These aliquots were subsequently subjected to ICP testing. The results reveal that only a trace amount of leached Cu (approximately 0.1 ppm) was detected in the electrolyte after each hour of reaction. Most importantly, the concentration of leached Co species consistently remained below the instrumental detection limit across all tested aliquots (**Table R1**). The ICP results reveal that the concentration of leached Co species in the post-reaction electrolyte is negligible. The combination of the persistent solid-state CoN_4 coordination and the absence of liquid-phase dissolved Co provides evidence that the TCPP(Co) molecules are resistant to demetallation and leaching under operational electrocatalytic conditions.

We have added the post-reaction XPS spectra to the Supporting Information and updated the corresponding discussion in the revised manuscript.

Table. R1 | Quantitative ICP analysis of leached metal concentrations in the electrolyte during continuous electrocatalysis.

Electrolysis time (h)	Cu Concentration (ppm)	Co Concentration (ppm)
1	~ 0.10	Undetected
2	~ 0.10	Undetected
3	~ 0.10	Undetected
4	~ 0.10	Undetected
5	~ 0.10	Undetected

Corresponding revision:

❑ The modification has been highlighted in **Page [10], Line [251]** of the revised main text: [Moreover, post-stability test analyses demonstrate the robust nature of the catalyst. XPS spectra verify the sustained presence of the Co centers, and HRTEM images reveal the intact amorphous molecular overlayer, confirming the preservation of the molecular-metal interface during prolonged operation (**Supplementary Fig. 22**).]

❑ To provide a more cohesive presentation of these results, we have integrated **Fig. R1** and **Fig. R8** into a single figure. This new figure has been added to the revised Supplementary Information as **Supplementary Figure 22**.

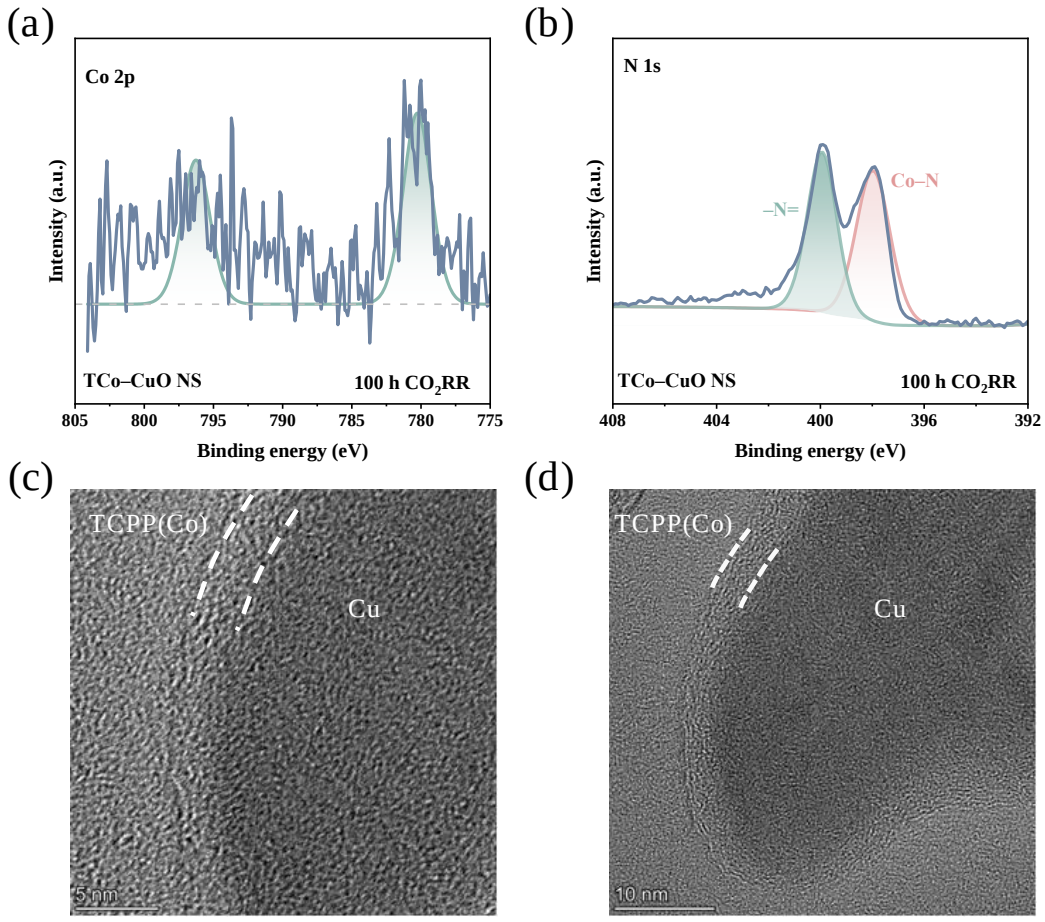

Supplementary Figure 22. High-resolution XPS spectra of TCo-CuO NS (a) Co 2p and (b) N 1s. (c, d) HRTEM image of TCo-CuO NS, the thin layer of TCPP(Co) was marked by white line, after 100 h stability test at 0.2 A cm^{-2}.

2. The control samples are insufficient, FE data for samples modified with only the organic molecules (without the metal center) should be added.

Response: We sincerely thank the reviewer for pointing out this control experiment. We completely agree that evaluating a metal-free organic molecule control is essential to unambiguously demonstrate the indispensable role of the Co metal center in our proposed dual-site synergistic mechanism. Following your highly constructive suggestion, we synthesized a new control sample using the metal-free based porphyrin (denoted as H_2TCPP–CuO NS) under identical preparation conditions. We then evaluated its CO_2RR performance under the exact same acidic conditions (pH 2, 1 M KCl electrolyte) (**Fig. R2**).

Corresponding revision:

❑ The modification has been highlighted in **Page [13], Line [334]** of the revised main text: [In contrast, incorporation of TCPP(Co) markedly enhances C–C coupling efficiency compared with TCu–CuO NS, TAg–CuO NS, TNi–CuO NS and CuO NS modified with H_2TCPP (H_2TCPP–CuO NS) (**Supplementary Fig. 36a to e**).]

❑ We have incorporated the control data presented in **Fig. R2** into **Figure 3d** and **Supplementary Figure 36** of the revised Supplementary Information. Furthermore, we have updated the corresponding discussion in the main text to reflect these additions:

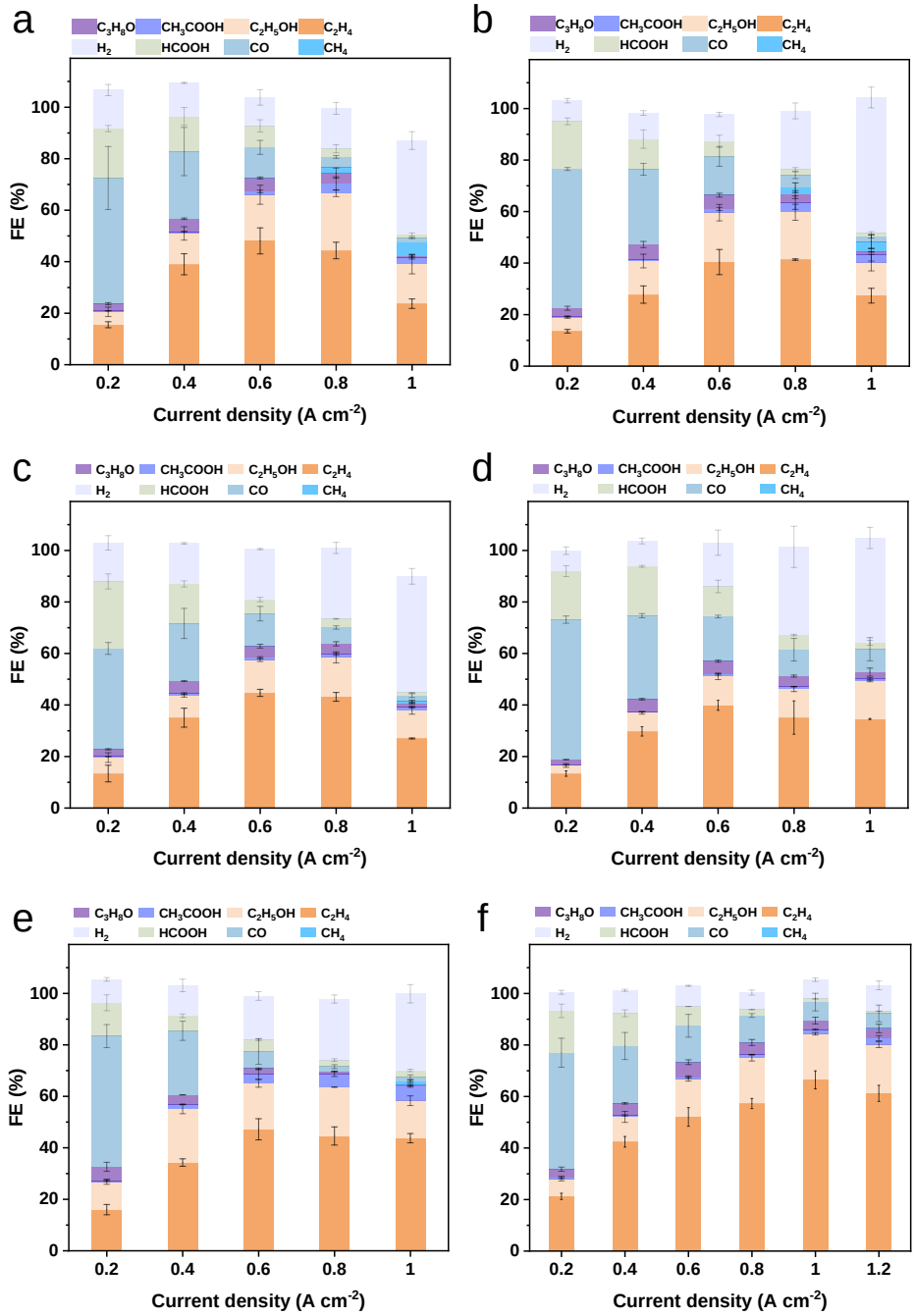

Fig. R2 | The CO_2RR product distributions obtained at different current densities **a,** TCu–CuO NS, **b,** TAg–CuO NS, **c,** TNi–CuO NS, **d,** CuO NS, **e,** H_2TCPP–CuO NS, and **f,** TCo–CuO NS in the presence of 1 M KCl at pH 2.

3. Although in situ EPR successfully captured the ·H signal, to prove that ·H is indeed directly involved in CO_2 activation and hydrogenation (rather than in an unrelated, parallel side reaction), the authors should perform a radical quenching experiment. It is recommended to add a specific hydrogen radical scavenger (such as DMPO or

other suitable trapping agents) to the electrolyte and observe whether the FE of C_{2+} drops significantly.

Response: We thank the reviewer for this insightful and constructive suggestion. We completely agree that while in situ electron paramagnetic resonance (EPR) confirms the presence of transient ·H radicals, a radical quenching experiment is strictly necessary to establish a definitive causal relationship between these radicals and the generation of C_{2+} products, thereby ruling out the possibility of an unrelated parallel side reaction. Encouraged by your constructive advice, to provide definitive evidence that the ·H captured by in situ EPR is directly involved in the CO_2 activation and hydrogenation pathway, we performed a radical quenching experiment using 5,5-dimethyl-1-pyrroline N-oxide (DMPO) as a hydrogen radical scavenger. Specifically, the CO_2RR was conducted in 40 mL of 1 M KCl (pH 2) electrolyte. At the 200-second mark of the reaction, 100 μL of DMPO was injected into the electrolyte, followed by immediate sampling for gas chromatography analysis. The experimental results reveal a significant decrease in the FE for C_{2+} products upon the addition of DMPO compared to the control experiment without the scavenger (**Fig. R3**). This marked drop in C_{2+} selectivity clearly demonstrates that the availability of ·H is a prerequisite for the efficient formation of C_{2+} species. This observation provides compelling evidence that ·H acts as a critical intermediate in the activation of CO_2 or the hydrogenation of *CO to *CHO.

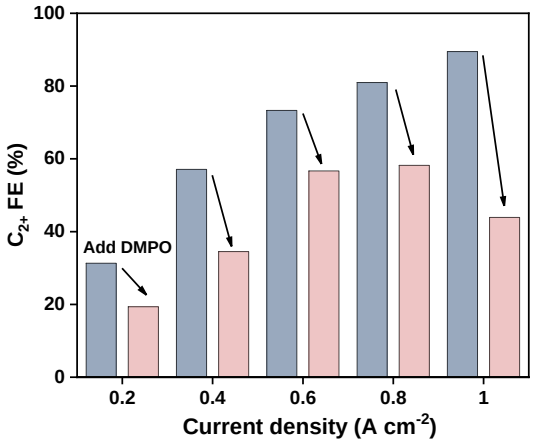

Fig. R3 | Comparison of C_{2+} FE over the TCo–CuO NS catalyst with and without the addition of DMPO.

Corresponding revision:

❑ The modification has been highlighted in **Page [17], Line [433]** of the revised main text: [The direct necessity of ·H in this pathway was further corroborated by a radical quenching experiment; the injection of a DMPO scavenger during continuous CO_2RR induced a significant drop in C_{2+} FE (**Supplementary Fig. 51**), definitively confirming that ·H is an essential intermediate for C_{2+} product formation rather than a byproduct of a parallel side reaction.]

❑ We have incorporated the control data presented in **Fig. R3** into **Supplementary Figure 51** of the revised Supplementary Information.

4. Regarding the use of PTFE instead of carbon paper in the stability tests, a specific and detailed implementation procedure should be provided in the Experimental section.

Response: We sincerely thank the reviewer for this constructive suggestion. We agree that providing a detailed procedure for the use of the polytetrafluoroethylene (PTFE) membrane is essential for the transparency and reproducibility of our long-term stability tests.

The primary motivation for replacing conventional carbon paper with a double-sided hydrophobic PTFE membrane was to fundamentally eliminate the adverse effects associated with carbon paper. Under prolonged electrolysis and applied potential, traditional carbon paper tends to undergo structural degradation and become hydrophilic, which inevitably leads to electrolyte flooding and performance decay. To visually demonstrate the effectiveness of this modification, we have provided an actual photograph of the internal local structure of the gas diffusion electrode after 100 h continuous stability test (**Fig. R4**). As clearly shown in the image, no water droplets or signs of flooding were observed within the PTFE layer, confirming its excellent and sustained hydrophobicity during long-term operation.

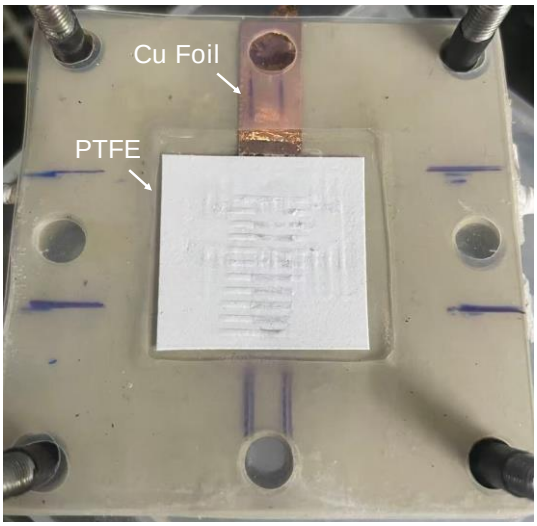

Fig. R4 | Photograph of the Flow Cell assembly and the PTFE gas diffusion layer after 100 hours of long-term stability test.

Furthermore, as requested, we have added a specific and detailed step-by-step implementation procedure for the preparation and assembly of the PTFE-based electrode in the Experimental section of the revised manuscript.

Corresponding revision:

❑ The modification has been highlighted in **Page [27], Line [692]** of the revised main text: [**Fabrication of GDE for Long-term Stability Tests**

The composite gas diffusion electrode was prepared by uniformly depositing the well-dispersed catalyst ink onto a piece of carbon paper, which served as the first layer. A double-sided hydrophobic PTFE membrane was then placed tightly against the uncoated back side of the carbon paper as the second layer. A copper foil was placed in direct physical contact with the carbon paper layer to serve as the current collector. Finally, the integrated composite electrode was mounted into the flow cell electrolyzer, with the catalyst-coated side of the carbon paper facing the aqueous catholyte and the PTFE membrane facing the gas chamber.]

5. Comparative EPR analysis between TAg–CuO NS and bare CuO NS under a CO_2 atmosphere is missing.

Response: We sincerely thank the reviewer for pointing out this control experiment. We completely agree that a directly comparative EPR analysis under identical in situ working conditions is strictly necessary to unambiguously demonstrate the unique role of the TCPP(Co) modifier in generating and stabilizing the crucial ·H radicals. Following your insightful suggestion, we have performed the corresponding in situ EPR measurements on the bare CuO NS and TCPP(Ag)–CuO NS control sample. The experiments were strictly conducted under the same acidic conditions and applied potentials, using the same radical spin trap.

Based on these two spectra, both control samples exhibit a highly similar (**Fig. R5**). Comparison with the EPR spectra of TCo–CuO nanostructures reveals the most notable difference **(Fig. 4b)**, the absence of the typical ·H signal with its characteristic doublet splitting. Instead, the formation of CO_2· or other surface radical intermediates associated with CO_2 activation is more likely. These experimental results further demonstrate that the Co metal center in TCPP(Co) plays a crucial role in the generation of ·H.

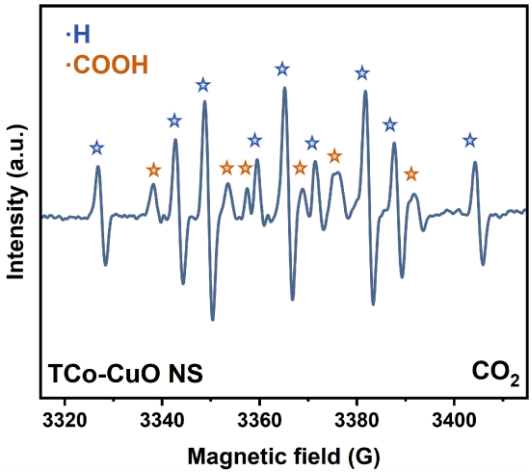

Fig. 4b | In situ EPR spectra recorded in pH 2, 1 M KCl electrolyte under CO_2 atmosphere using DMPO as a trapping reagent, after 10 min of CO_2RR on TCo–CuO NS.

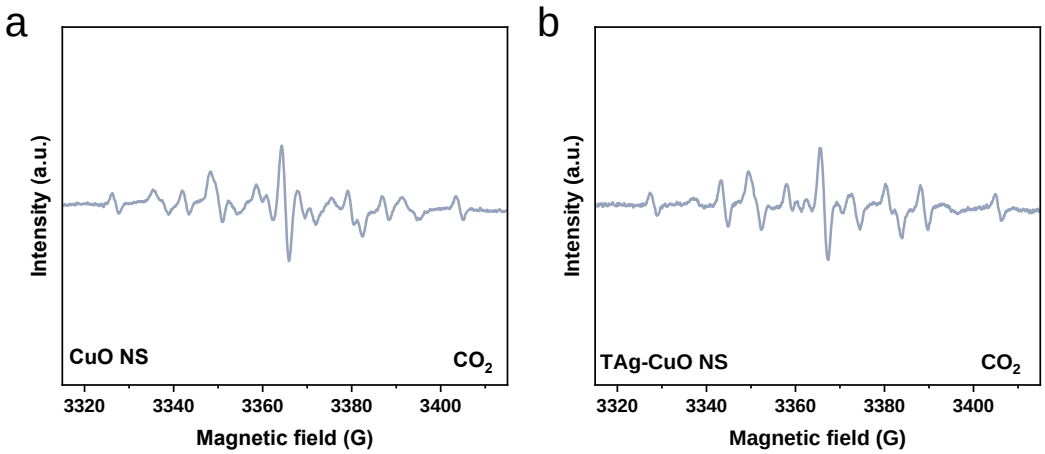

Fig. R5 | In situ EPR spectra recorded in pH 2, 1 M KCl electrolyte under CO_2 atmosphere using DMPO as a trapping reagent, after 10 min of CO_2RR on **a,** CuO NS and **b,** TAg–CuO NS.

Corresponding revision:

❑ The modification has been highlighted in **Page [16], Line [430]** of the revised main text: [Furthermore, comparative in situ EPR measurements of bare CuO NS and TAg–CuO NS under the same CO_2 atmosphere confirm the complete absence of this characteristic ·H signal (**Supplementary Fig. 50**), unambiguously demonstrating that the Co metal center in TCPP(Co) is indispensable for generating the crucial ·H radicals.]

❑ The information presented in **Fig. R5** has been used as **Supplementary Figure 50** in the revised Supplementary Information.

6. The current DFT analysis appears to focus primarily on energetics. To provide a deeper understanding of why H* readily spills over from the Co site, an electronic structure analysis is recommended. The authors should calculate and analyze the electron density of states, charge density difference, or Crystal Orbital Hamilton Population (COHP) for H-adsorption on the Co site. This could explain the thermodynamic and/or kinetic factors that favor the detachment of H* from the Co center.

Response: We thank the reviewer for this constructive suggestion. We fully agree that

electronic structure analysis is crucial for understanding the intrinsic driving force behind H* spillover from the Co center. Accordingly, we have performed comprehensive electronic structure calculations, including charge density difference, Bader charge analysis, and Crystal orbital hamilton population (COHP) analysis for the Co–H configuration. The differential charge density plot (**Fig. R6**) reveals significant electron redistribution upon H adsorption on Co. Bader charge analysis quantifies an electron transfer of ~0.06 e^- from H to Co, indicating a polarized Co–H bond with partial hydridic character ($H^{\delta+}$). This electron deficiency at the Co center and the resulting Coulombic repulsion contribute to the thermodynamic driving force for H* detachment and migration toward the more electronegative Cu surface or porphyrin nitrogen atoms.

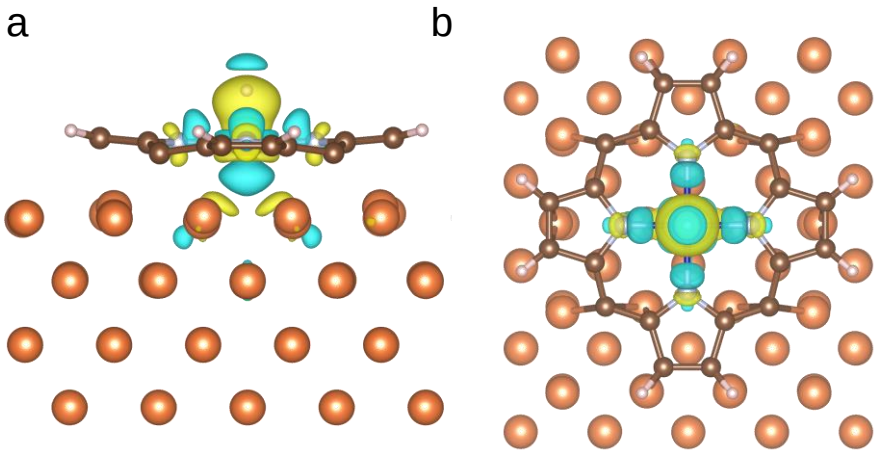

Fig. R6 | (a) Side and (b) top views of the charge density difference for the Co–porphyrin–H configuration. Yellow and cyan isosurfaces represent regions of electron accumulation and depletion, respectively.

To evaluate the Co–H bond strength, we calculated the COHP for the Co–H interaction. The integrated COHP (ICOHP) up to the Fermi level is 1.06. This moderate Co–H interaction is consistent with the facile H* spillover observed in our thermodynamic calculations (**Fig. R7**). The electronic structure thus provides a fundamental rationale for the kinetic accessibility and thermodynamic favorability of the proposed hydrogen transfer mechanism.

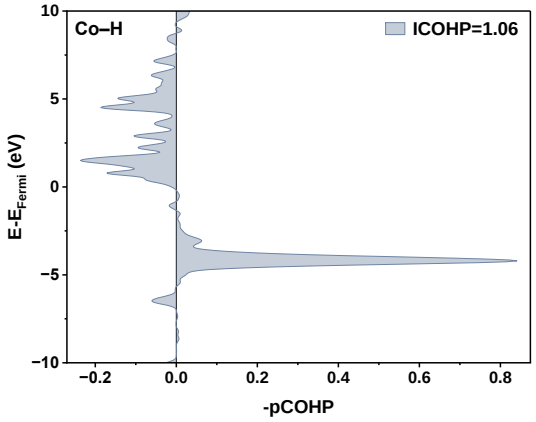

Fig. R7 | Crystal Orbital Hamilton Population (-pCOHP) and ICOHP profiles for the Co–H bond.

Corresponding revision:

❑ The modification has been highlighted in **Page [6], Line [143]** of the revised main text: [To elucidate the intrinsic mechanism of H* spillover from the Co site, comprehensive electronic structure analyses were performed. Differential charge density and Bader charge calculations reveal an electron transfer of ~0.06 e^- from H to Co. The resulting polarized Co–H bond ($H^{\delta+}$) induces Coulombic repulsion, providing the thermodynamic driving force for H* migration toward the more electronegative Cu surface or porphyrin nitrogen atoms. Furthermore, Crystal Orbital Hamilton Population (COHP) analysis yields an integrated COHP (ICOHP) of 1.06 up to the Fermi level. This moderate Co–H bond strength facilitates initial H adsorption without causing excessive stabilization, fundamentally rationalizing the kinetic accessibility and thermodynamic favorability of the H* spillover, Specifically, free energy profiling of the spillover pathway demonstrates that, despite a minor initial uphill step toward the porphyrin nitrogen (0.28 eV), the overall migration of *H from the Co center to the Cu surface is thermodynamically downhill with a net driving force of –0.76 eV, enabling it to readily participate in the subsequent hydrogenation of *CO to *CHO (**Supplementary Fig. 5 and Supplementary Note 1**).]

❑ To provide a more cohesive presentation of these results, we have integrated **Fig. R6, Fig. R7,** and **Fig. R10** into a single figure. This new figure has

been added to the revised Supplementary Information as **Supplementary Figure 5**.

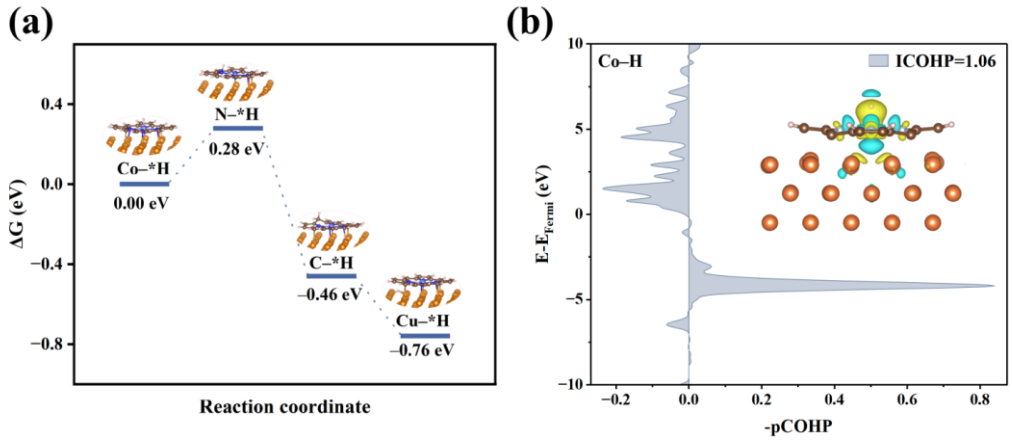

Supplementary Figure 5. (a) Free energy profile for the hydrogen spillover pathway. (b) The crystal orbital hamilton population (-pCOHP) and ICOHP profiles for the Co–H bond; and side views of the charge density difference for the Co–porphyrin–H configuration. Yellow and cyan isosurfaces represent regions of electron accumulation and depletion, respectively.

Supplementary Note 1: The free energy step diagram depicts a plausible hydrogen spillover pathway, illustrating the sequential migration of the adsorbed H species from the Co center to an adjacent pyrrolic N atom, subsequently to a C atom of the porphyrin ring, and ultimately onto the Cu substrate. This step-wise energetic analysis demonstrates the thermodynamic feasibility of the H spillover process.

7. In Supplementary Fig. 33, the y-axis is labeled "Yield (mmol h^{-1} cm^{-2})". In chemistry, "Yield" is usually a percentage value; using "Production rate" or "Formation rate" would be scientifically more accurate.

Response: We highly appreciate the reviewer for pointing out this terminology inaccuracy with such carefulness. We completely agree that "Production rate" (or "Formation rate") is the scientifically rigorous term for the unit mmol h^{-1} cm^{-2}, as "Yield" is conventionally used to represent a percentage value in chemistry. Following your precise suggestion, we have carefully thoroughly checked the entire manuscript and updated the y-axis labels from "Yield" to "Production rate" in Supplementary Fig. 37.

Accordingly, we have also corrected the corresponding text descriptions throughout

the revised manuscript to ensure strict scientific accuracy and consistency.

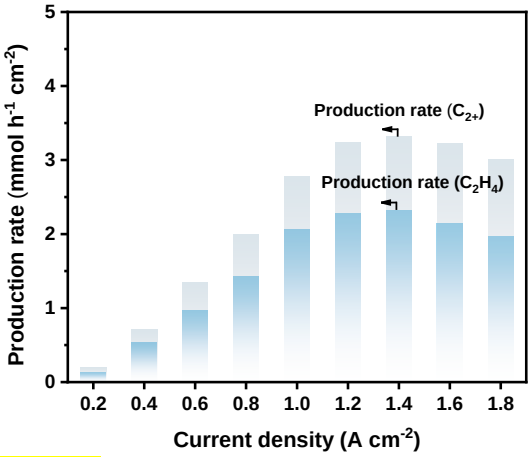

Revised Fig. S37 | Production rate of C_2H_4 and C_{2+} products for TCo–CuO NS calculated based on FEs.

8. In the main text, when mentioning that the Δν of the -COO stretching vibration "decreased from 209 cm^{-1} to 171 cm^{-1}", "Supplementary Fig. 16" should be directly cited in that specific sentence to ensure the clarity of the text.

Response: We highly appreciate your exceptionally careful reading and helpful suggestion to improve the flow and clarity of our manuscript. We completely agree that directly citing the specific figure right where the corresponding numerical data is discussed is crucial for readers.

Following your precise instruction, we have immediately added the citation for **Supplementary Fig. 18** (formerly **Supplementary Fig. 16**) into that specific sentence. Furthermore, we have carefully thoroughly proofread the entire manuscript to ensure all corresponding figures are accurately and timely cited whenever specific data points or spectroscopic shifts are mentioned.

Corresponding revision:

❑ The modification has been highlighted in **Page [9], Line [242]** of the revised main text: [Post-CO_2RR ATR-FTIR analysis demonstrates the persistence of surface -COO^- groups after in situ electroreduction (**Supplementary Fig. 18a and 18b**). The separation between asymmetric and symmetric -COO^- stretching modes (Δν)

decreases from 209 cm^{-1} to 171/178 cm^{-1}, indicative of a dynamic structural evolution into a highly stable bidentate coordination between in situ generated metallic Cu and TCPP(Co), which is computationally verified to be thermodynamically more stable than the monodentate mode by 0.35 eV (**Supplementary Fig. 18c and 18d**).]

Reply to Reviewer #2:

In this manuscript, Jin et al. presents a highly interesting and thoroughly investigated strategy to achieve efficient multicarbon (C_{2+}) product generation in acidic CO_2 electroreduction (CO_2RR). By anchoring the molecular modifier TCPP(Co) onto CuO nanosheets, the authors constructed a dual-site synergistic interface. The manuscript convincingly demonstrates that TCPP(Co) can regulate the proton transfer pathway by promoting the formation of transient hydrogen radicals and disrupting the interfacial water network, thereby facilitating asymmetric *CHO–*CO coupling on adjacent Cu sites while suppressing the competing hydrogen evolution reaction (HER). The catalyst achieved a highly competitive C_{2+} Faradaic efficiency of 89.5% at a high current density of 1 A cm^{-2} in a pH 2 electrolyte. Furthermore, the combination of in situ EPR, in situ SERS, AIMD, and static DFT provides multi-dimensional mechanistic insights. The manuscript is logically rigorous, and its results will be highly appealing to a broad readership in the fields of electrocatalysis and energy conversion. After the authors address the following minor concerns and clarify the related details, I believe this manuscript will fully meet the publication standards of *Nature Communications*. I recommend accepting it after minor revisions.

Response: We would like to express our deepest gratitude to the reviewer for the exceptionally positive evaluation, thorough reading, and insightful summary of our manuscript. We are thrilled and deeply encouraged that you find our strategy for achieving efficient multicarbon (C_{2+}) product generation in acidic CO_2RR to be highly interesting and thoroughly investigated. It is incredibly rewarding to receive your strong recognition of our proposed dual-site synergistic mechanism. We are delighted that our multi-dimensional mechanistic insights—combining in situ Electron paramagnetic resonance (EPR), in situ surface-enhanced Raman spectroscopy (SERS), ab initio molecular dynamics (AIMD), and static density functional theory (DFT) to elucidate how the TCPP(Co) modifier regulates the proton transfer pathway and disrupts the interfacial water network—are viewed as logically rigorous. We are equally encouraged by your positive appraisal of our catalytic performance. We also deeply appreciate your constructive minor concerns. We fully agree that addressing these points and clarifying the related details are essential steps to further refine the

manuscript and ensure it perfectly meets the publication standards of ***Nature Communications***. In accordance with your valuable suggestions, we have carefully considered each point and made the corresponding revisions. Please find our detailed, point-by-point responses to your specific comments below.

1. Quantitative analysis of catalyst loading. The authors mentioned concentration dependent performance (e.g., excessively coated TCo–CuO NS-3 led to decreased ECSA and performance due to the masking of active sites). However, absolute loading data for TCPP(Co) on the optimally performing TCo–CuO NS is not provided. It is recommended to provide data to precisely quantify the atomic ratio of Co/Cu.

Response: We sincerely thank the reviewer for pointing out this critical omission. We completely agree that providing quantitative atomic ratio data is essential for fundamentally understanding the concentration-dependent performance and the optimal dual-site balance at the catalyst interface.

Since electrocatalytic reactions exclusively occur on the catalyst surface, we have performed semi-quantitative X-ray photoelectron spectroscopy (XPS) analysis to precisely determine the surface atomic ratio of Co to Cu, which directly dictates the interfacial catalytic behavior, alongside inductively coupled plasma optical emission spectrometry (ICP-OES) measurements to determine the bulk absolute loading.

Specifically, based on our initial precursor feed (3 mg TCPP(Co) and 30 mg CuO), the theoretical bulk Co/Cu atomic ratio is calculated to be approximately 0.94% (a molar ratio of roughly 1:106) (**Table R2**). However, to determine the precise absolute loading, we conducted ICP-OES measurements. The results reveal that the actual bulk Co/Cu atomic ratio for the optimal 1× sample is 0.50% (Cu:Co = 199:1). While this actual bulk loading is lower than the theoretical precursor feed, this deviation is highly reasonable and expected in surface immobilization strategies. It is attributed to the thorough washing and centrifugation processes during synthesis, which effectively remove the unanchored or weakly physisorbed TCPP(Co) molecules, leaving only the robustly chemisorbed active species on the CuO surface.

Despite the low bulk loading, high-resolution XPS analysis of this optimal TCo–

CuO NS reveals a surface Co proportion of 3.37%. This substantial discrepancy between the surface concentration (3.37%) and the actual bulk loading (0.50%) provides direct, quantitative proof of the successful surface enrichment and structural anchoring of the TCPP(Co) molecules strictly at the interface.

To further explain the concentration-dependent performance, we analyzed the excessively coated TCo–CuO NS-3 sample. ICP-OES results show that despite a three-fold increase in the precursor feed, the actual bulk Co/Cu ratio only slightly increased to 0.64% (Cu:Co = 157:1). This indicates that the available chemical anchoring sites on the CuO surface approach saturation. Consequently, the excessive TCPP(Co) inevitably piles up at the interface. This is corroborated by the XPS results of the 3× sample, which show a substantially increased surface Co ratio of 3.99%. This combined ICP and XPS quantitative data provides compelling evidence for our hypothesis: excessive TCPP(Co) loading leads to severe physical masking of the intrinsic Cu active sites, which inevitably decreases the ECSA and the overall CO_2RR performance.

Furthermore, to evaluate the structural robustness, we quantified the surface Co ratio of the optimal sample after 100 h stability test. The XPS analysis demonstrates that the surface Co content only experienced a minor decrease from 3.37% to 2.75% (**Table R3**). This minimal change confirms that the Co species do not suffer from severe detachment or dissolution during prolonged electrocatalysis.

Table. R2 | Theoretical and actual bulk Co/Cu atomic ratios of the optimal (1×) and excessively loaded (3×) TCo–CuO NS catalysts determined by ICP-OES.

Samples	Theoretical Co/Cu atomic ratio	Co/Cu atomic ratio
TCo–CuO NS	0.94%	0.50%
TCo–CuO NS-3	2.82%	0.64%

Table. R3 | Detailed fitting position of TCo–CuO NS and TCo–CuO NS (Post CO_2RR) based on high-resolution XPS spectra.

Catalysts	Cu 2p Fitting position (eV)	Co 2p Fitting position (eV)	Atomic ratio Cu:Co
TCo–CuO NS	934.70/954.51	780.42/795.35	96.63:3.37
TCo–CuO NS (Post CO_2RR)	934.45/954.38	780.47/795.42	97.25:2.75
TCo–CuO NS-3	934.58/954.35	779.75/794.72	96.01:3.99

Corresponding revision:

❑ The modification has been highlighted in **Page [10], Line [264]** of the revised main text: [To determine the precise absolute loading, inductively coupled plasma optical emission spectrometry (ICP-OES) was performed, revealing an actual bulk Co/Cu atomic ratio of 0.50% (**Supplementary Table 2**). Crucially, semi-quantitative XPS analysis reveals a surface Co proportion of 3.37%, significantly exceeding the theoretical bulk ratio (~0.94%), which directly confirms the successful surface enrichment and molecular anchoring of TCPP(Co) (**Supplementary Table 3**).]

❑ We have incorporated all these quantitative ICP and XPS results into **Supplementary Table 2 and 3** of the revised Supplementary Information, and updated the corresponding discussion in the main text:

2. Figure 3g demonstrates excellent 100-hour stability at 0.2 A/cm². Although the authors provided post-reaction characterizations (ATR-FTIR, TEM) after short-term testing, confirming the stability of the molecular modifier after the 100-hour test is crucial. It is recommended to perform post-reaction XPS and ATR-FTIR characterizations on the electrode after prolonged continuous electrolysis. This would strongly prove that the porphyrin macrocycle does not degrade or detach under prolonged cathodic polarization.

Response: We sincerely appreciate the reviewer's highly constructive suggestion. We completely agree that providing post-reaction characterizations after the 100-hour continuous electrolysis is essential to definitively prove the structural robustness of the molecular modifier under prolonged cathodic polarization. Following your recommendation, we have performed the requested XPS, high-resolution transmission electron microscopy (HRTEM), and attenuated total reflection Fourier transform infrared spectroscopy (ATR-FTIR) analyses on the post-100 h electrode, and the results strongly confirm that the porphyrin macrocycle neither degrades nor detaches.

We acquired the Co 2p and N 1s high-resolution XPS spectra of the post-100 h sample (**Fig. R1**). These spectra perfectly match those of the pristine catalyst, with no emergence of zero-valent Co or CoO species, confirming that the Co–N_4 coordination centers remain highly stable under prolonged cathodic polarization.

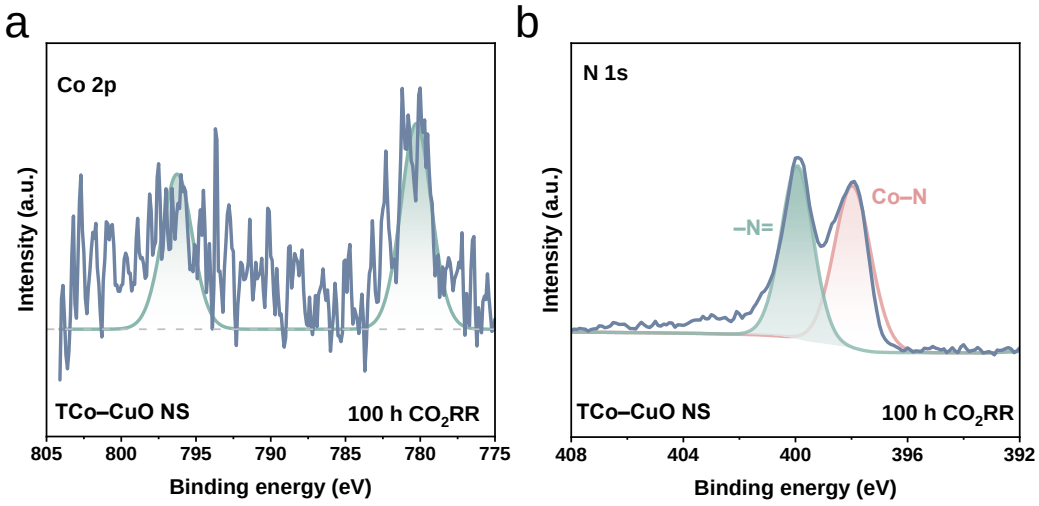

Fig. R1 | High-resolution XPS spectra of the catalyst after 100 h stability test at 0.2 A cm^{-2}, **a,** Co 2p and **b,** N 1s.

To provide even more comprehensive proof, we also supplemented post-100 h HRTEM imaging, which shows the preserved nanoscale molecular layer (**Fig. R8**). Along with an accelerated continuous ICP leaching test to further corroborate the excellent anchoring stability of TCPP(Co).

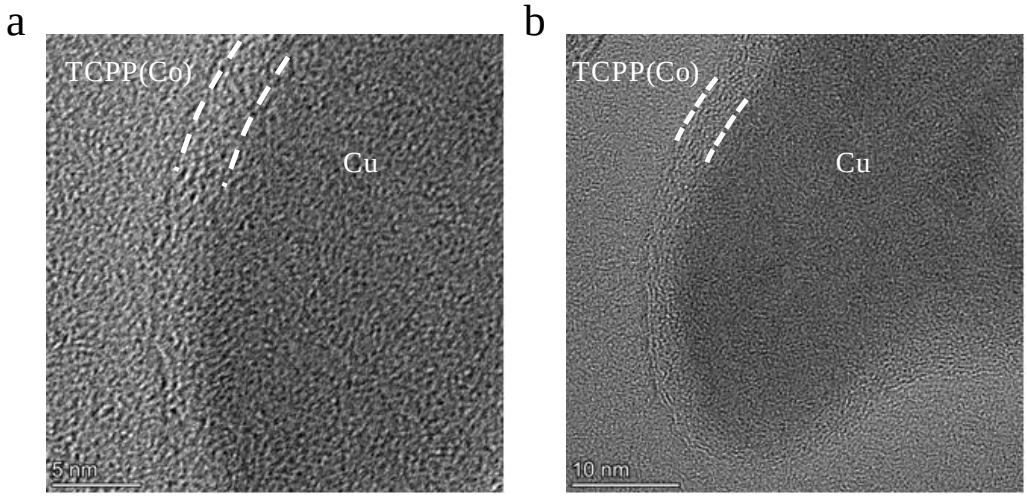

Fig. R8 | HRTEM image of TCo–CuO NS after 100 h CO_2RR, the thin layer of TCPP(Co) was marked by white line.

Consistently, the post-reaction ATR-FTIR spectrum (**Fig. R9**) shows that the characteristic Δv of the -COO^- stretching vibrations remains largely unchanged, confirming that the molecules remain strongly anchored to the Cu surface via the bidentate coordination without detaching (***Coordination Chemistry Reviews***, 1980, 33, 3, 227-250).

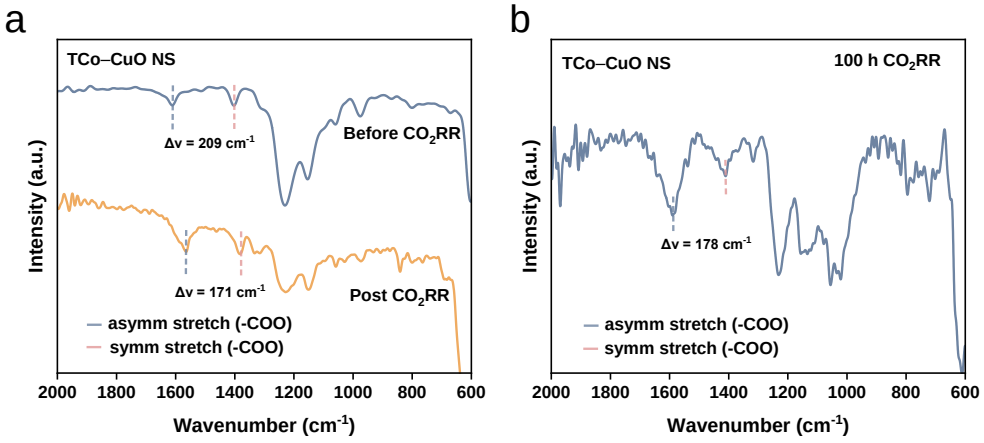

Fig. R9 | ATR-FTIR spectra of TCo–CuO NS **a,** before, after 3 h CO_2RR test and **b,** after 100 h CO_2RR test at 0.2 A cm^{-2}.

Corresponding revision:

❑ The modification has been highlighted in **Page [10], Line [249]** of the revised

main text: [The uniform distribution of TCPP(Co) on the CuO NS is evident prior to the reaction (**Supplementary Fig. 19)** and is maintained after CO_2RR, as confirmed by energy-dispersive X-ray spectroscopy (EDS) elemental mapping (**Supplementary Fig. 20**). Moreover, post-stability test analyses demonstrate the robust nature of the catalyst. High-angle annular dark-field scanning transmission electron microscopy (HAADF-STEM) EDS elemental mapping confirms the persistent uniform dispersion of the Co species after 100 h of continuous operation (**Supplementary Fig. 21**). XPS spectra verify the sustained presence of the Co centers (**Supplementary Fig. 22a-22b and Supplementary Note 2**), and HRTEM images reveal the intact amorphous molecular overlayer, confirming the preservation of the molecular-metal interface during prolonged electrolysis (**Supplementary Fig. 22c-22d and Supplementary Note 3**).]

❑ The modification has been highlighted in **Page [9], Line [242]** of the revised main text: [Post-CO_2RR ATR-FTIR analysis demonstrates the persistence of surface –COO^- groups after in situ electroreduction (**Supplementary Fig. 18a and 18b**). The separation between asymmetric and symmetric –COO^- stretching modes ($\Delta\nu$) decreases from 209 cm^{-1} to 171/178 cm^{-1}, indicative of a dynamic structural evolution into a highly stable bidentate coordination between in situ generated metallic Cu and TCPP(Co)[37], which is computationally verified to be thermodynamically more stable than the monodentate mode by 0.35 eV (**Supplementary Fig. 18c and 18d**).]

❑ To provide a more cohesive presentation of these results, we have integrated **Fig. R1** and **Fig. R8** into a single figure. This new figure has been added to the revised Supplementary Information as **Supplementary Figure 22**.

❑ To provide a more cohesive presentation of these results, we have integrated **Fig. R9** and **Fig. R14** into a single figure. This new figure has been added to the revised Supplementary Information as **Supplementary Figure 18**.

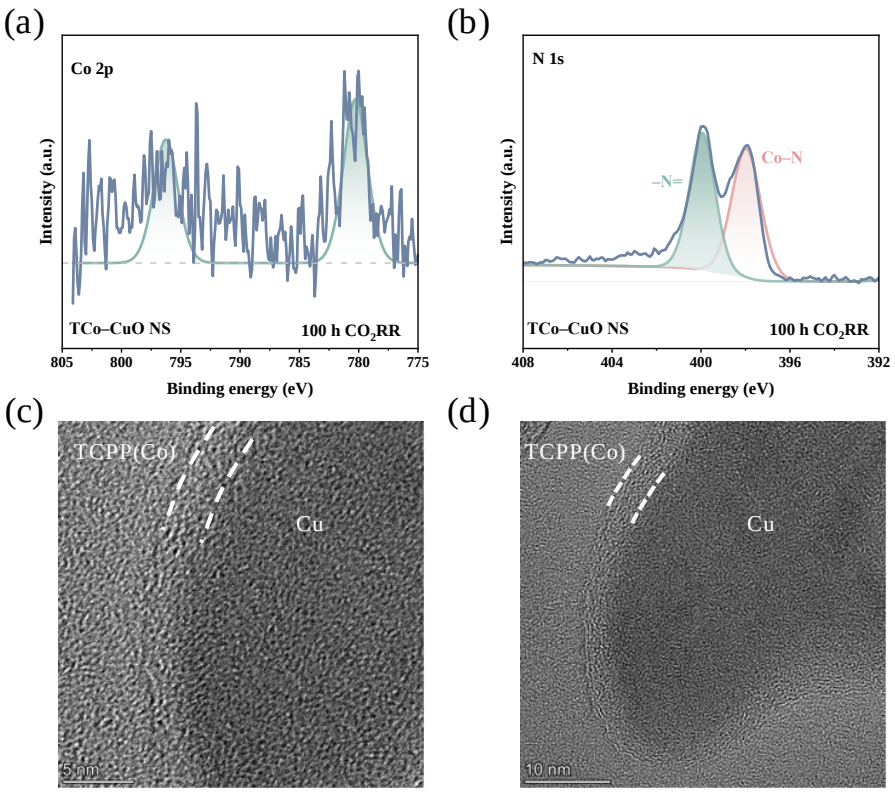

Supplementary Figure 22. High-resolution XPS spectra of TCo-CuO NS (a) Co 2p and (b) N 1s. (c, d) HRTEM image of TCo-CuO NS, the thin layer of TCPP(Co) was marked by white line, after 100 h stability test at 0.2 A cm^{-2}.

Supplementary Note 2: We acquired the Co 2p and N 1s high-resolution XPS spectra of the post-100 h sample (**Supplementary Figure 22a-22b**). These spectra perfectly match those of the pristine catalyst, with no emergence of zero-valent Co or CoO species, confirming that the Co–N_4 coordination centers remain highly stable under prolonged cathodic polarization.

Supplementary Note 3: To provide even more comprehensive proof, we also supplemented post-100 h HRTEM image, which shows the preserved nanoscale molecular layer (**Supplementary Figure 22c-22d**). Along with an accelerated continuous ICP leaching test to further corroborate the excellent anchoring stability of TCPP(Co).

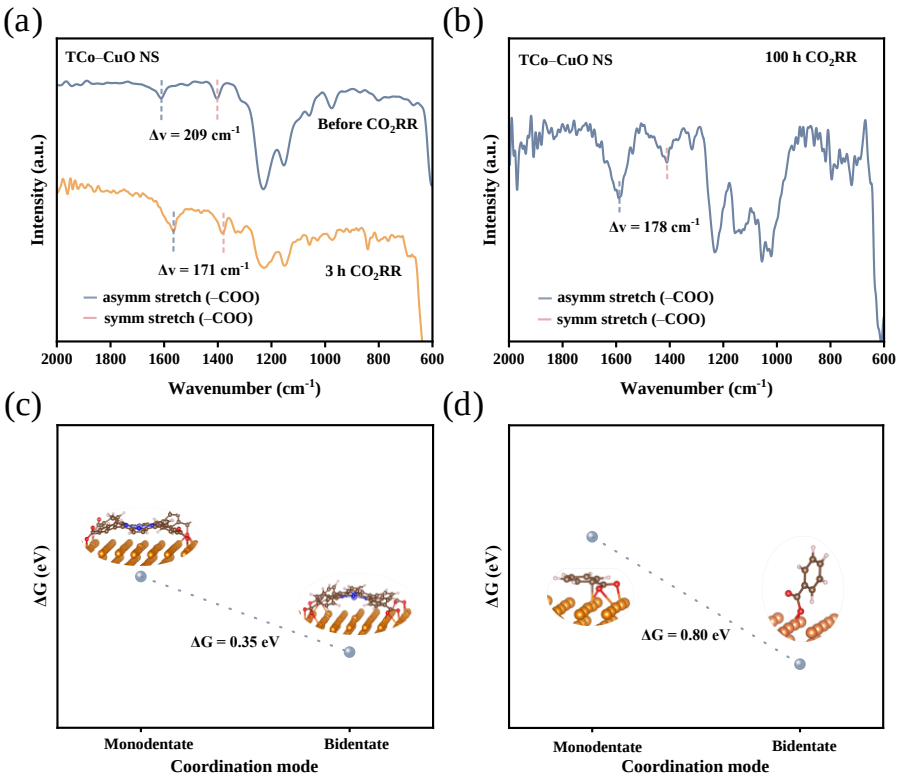

Supplementary Figure 18. ATR-FTIR spectra of TCo-CuO NS (a) before and after 3 h CO_2RR test, (b) after 100 h CO_2RR test at 0.2 A cm^{-2}. Calculated relative free energy (ΔG) profiles comparing the monodentate and bidentate configurations for (c) the simplified benzoic acid (BZA) model and (d) the complete TCPP(Co) complex. The bidentate coordination is thermodynamically preferred in both systems.

3. In the static DFT calculations (Figure 1), the authors use benzoic acid (BZA) to represent the TCPP(Co) modifier. While this is a reasonable simplification for studying the -COO-Cu electronic interaction, the BZA model lacks the bulky, hydrophobic porphyrin ring and the Co center. The authors should add a brief discussion or justification in the main text explaining why the BZA-Cu model is sufficient for describing the thermodynamics of C-C coupling. It should be explicitly stated that steric/hydrophobic effects and the Volmer step (H_2O dissociation on Co) are considered in the AIMD and/or unit-cell DFT calculations that utilize the full TCPP(Co) model, respectively.

Response: We thank the reviewer for the insightful comment regarding the use of benzoic acid (BZA) as a simplified model for the TCPP(Co) modifier. We agree that clarifying the rationale behind this modeling strategy is important for the

interpretation of the computational results. In response, we have added a brief discussion in the main text and provide further details below. To balance computational accuracy and feasibility, we adopted a tiered modeling approach.

For the thermodynamic analysis of the C–C coupling steps, BZA was employed as a simplified representation of the TCPP(Co) anchor. This simplification is fundamentally justified by their shared binding mechanism, as our structural optimizations confirm that the carboxylate groups in both the BZA model and the full TCPP(Co) complex adopt an identical bidentate coordination mode on the Cu(100) surface. Because the formation of C–C bonds is primarily governed by the local electronic structure at this –COO–Cu interface, the spatially separated porphyrin ring and Co center, which mainly influence molecule–surface interactions via van der Waals forces and electrostatic effects, which has a negligible impact on the intrinsic thermodynamics of the active site coupling steps. Consequently, utilizing the BZA model allows us to effectively isolate the electronic contribution of the carboxylate anchoring group without introducing additional non-local interactions, thereby enabling a cleaner and more focused evaluation of the reaction energetics directly relevant to C–C bond formation.

While this simplified model excludes the porphyrin ring and Co center, we note that steric and hydrophobic effects are fully accounted for in our AIMD simulations using the complete TCPP(Co) structure. Furthermore, the Volmer step (H_2O dissociation on Co) is explicitly evaluated in our calculations using the full TCPP(Co) model, where the reaction free energetics and hydrogen-bonding statistics are analyzed in detail (**Fig. 1c and Fig. 5a, b**).

Corresponding revision:

❑ The modification has been highlighted in **Page [4], Line [99]** of the revised main text: [For the thermodynamic analysis of C–C coupling, benzoic acid (BZA) was employed as a simplified anchoring ligand on the Cu(100) surface to maintain computational tractability. This simplification is highly justified, as the carboxylate–Cu coordination fundamentally modulates the local interfacial

electronic structure, whereas the spatially separated porphyrin macrocycle and metal center do not directly participate in Cu–C intermediate binding. Importantly, while the BZA–Cu(100) model is sufficient for describing the intrinsic coupling thermodynamics, the steric/hydrophobic effects of the bulky macrocycle and the Volmer step are explicitly accounted for in our ab initio molecular dynamics (AIMD) and unit-cell DFT calculations utilizing the full TCPP(Co) complex.]

4. The manuscript elegantly proposes the generation of H-radicals on TCPP(Co) that participate in the hydrogenation of *CO to *CHO on copper. However, the physical pathway for this hydrogen transfer (the spillover effect) remains ambiguous. The authors should at minimum provide a thermodynamic discussion of the energy required for the H-species to migrate from the Co center (or the porphyrin's N atoms) to the adjacent copper surface or to directly attack the adsorbed *CO.

Response: We thank the reviewer for raising this important point regarding the hydrogen spillover pathway from the TCPP(Co) center to the copper surface. We agree that clarifying the physical pathway for hydrogen transfer is essential for validating the proposed mechanism. To address this, we have performed additional thermodynamic analyses, which are summarized below.

We first evaluated the competitive adsorption of CO_2 and H_2O on the Co center of the TCPP(Co) complex. Our DFT calculations show that H_2O adsorbs more favorably than CO_2, with adsorption energies of –0.16 eV and –0.13 eV, respectively. This indicates that under reaction conditions, the Co center is preferentially occupied by H_2O, which can subsequently dissociate to generate *H species. To assess the energetics of hydrogen transfer from the Co center to the copper surface, we calculated the relative stabilities of *H at different sites along the spillover pathway. Using the *H species on the Co center (Co–H) as the reference state, we obtained the following energy changes (**Fig. R10**).

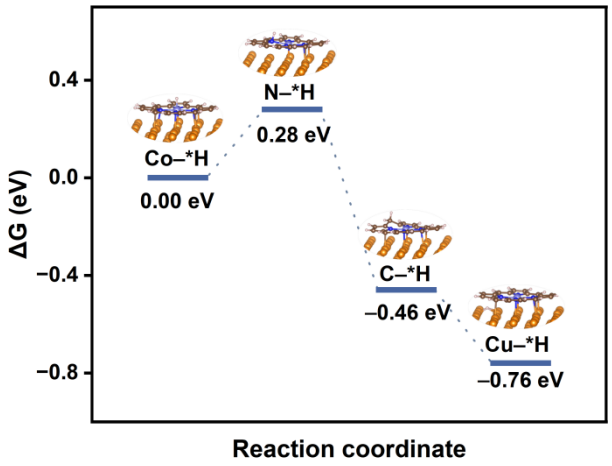

Fig. R10 | Free energy profile for the hydrogen spillover pathway.

Note: The free energy step diagram depicts a plausible hydrogen spillover pathway, illustrating the sequential migration of the adsorbed H species from the Co center to an adjacent pyrrolic N atom, subsequently to a C atom of the porphyrin ring, and ultimately onto the Cu substrate. This step-wise energetic analysis demonstrates the thermodynamic feasibility of the H spillover process.

Although a slight thermodynamic uphill step is encountered at the initial migration from Co to the porphyrin nitrogen, the overall hydrogen spillover process remains thermodynamically downhill, with a net driving force of –0.76 eV for transferring *H from the Co center to the Cu surface. Once on the copper surface, the *H species can readily participate in the hydrogenation of *CO to *CHO, which is a key step in the C–C coupling pathway.

Corresponding revision:

❑ The modification has been highlighted in **Page [6], Line [143]** of the revised main text: [To elucidate the intrinsic mechanism of H* spillover from the Co site, comprehensive electronic structure analyses were performed. Differential charge density and Bader charge calculations reveal an electron transfer of ~0.06 e^- from H to Co. The resulting polarized Co-H bond ($H^{\delta+}$) induces Coulombic repulsion, providing the thermodynamic driving force for H* migration toward the more electronegative Cu surface or porphyrin nitrogen atoms. Furthermore, Crystal

Orbital Hamilton Population (COHP) analysis yields an integrated COHP (ICOHP) of 1.06 up to the Fermi level. This moderate Co-H bond strength facilitates initial H adsorption without causing excessive stabilization, fundamentally rationalizing the kinetic accessibility and thermodynamic favorability of the H* spillover, Specifically, free energy profiling of the spillover pathway demonstrates that, despite a minor initial uphill step toward the porphyrin nitrogen (0.28 eV), the overall migration of *H from the Co center to the Cu surface is thermodynamically downhill with a net driving force of –0.76 eV, enabling it to readily participate in the subsequent hydrogenation of *CO to *CHO (**Supplementary Fig. 5 and Supplementary Note 1**).]

❑ To provide a more cohesive presentation of these results, we have integrated **Fig. R6, Fig. R7** and **Fig. R10** into a single figure. This new figure has been added to the revised Supplementary Information as **Supplementary Figure 5 and Supplementary Note 1**.

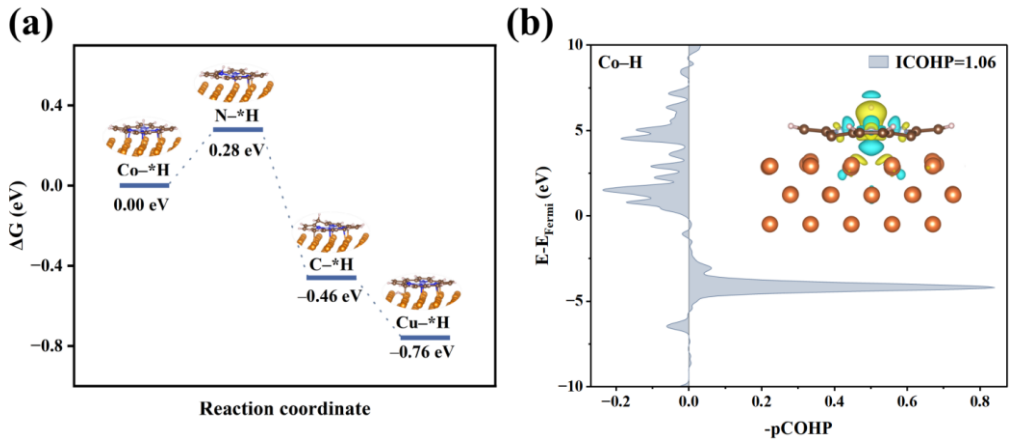

Supplementary Figure 5. (a) Free energy profile for the hydrogen spillover pathway. (b) The Crystal Orbital Hamilton Population (-pCOHP) and ICOHP profiles for the Co–H bond; and side views of the charge density difference for the Co–porphyrin–H configuration. Yellow and cyan isosurfaces represent regions of electron accumulation and depletion, respectively.

Supplementary Note 1: The free energy step diagram depicts a plausible hydrogen spillover pathway, illustrating the sequential migration of the adsorbed H species from the Co center to an adjacent pyrrolic N atom, subsequently to a C atom of the porphyrin ring, and ultimately onto the Cu substrate. This step-wise energetic analysis demonstrates the thermodynamic feasibility of the H spillover process.

5. In the mechanism discussion section, the manuscript sometimes conflates experimental observations from in situ characterizations (e.g., SERS/EPR) with theoretical deductions from AIMD/DFT within the same sentence. This makes it difficult for readers to quickly distinguish between directly observed facts and model-based inferences. I recommend using clearer transitional phrases and introductory words to bridge sentences and paragraphs.

Response: We highly appreciate the reviewer's constructive feedback regarding the writing flow and clarity of our mechanistic discussion. We completely agree that clearly distinguishing direct experimental facts from theoretical inferences is crucial for readers to accurately grasp the logical progression and scientific rigor of our study. Following your excellent recommendation, we have carefully revised and restructured the mechanism discussion section in the revised manuscript. We have systematically decoupled the descriptions of our empirical observations (in situ SERS and EPR) from the theoretical deductions derived from our computational models (AIMD and static DFT).

Furthermore, to ensure a seamless and unambiguous narrative, we have enriched the text with clear transitional phrases and specific introductory words. For instance, we now explicitly use phrases such as "which experimentally indicates that..." to present empirical facts, followed by clear bridges such as "Consistent with this theoretical picture, DFT calculations further revealed that..." or "According to our theoretical calculations,..." to introduce theoretical insights.

We believe that these text revisions have significantly improved the readability, logical clarity, and overall impact of the mechanistic discussion. The corresponding modifications have been highlighted throughout the **Investigation of electrocatalytic mechanism** section in the revised main text.

Corresponding revision:

❑ The modification has been highlighted in **Page [19], Line [487]** of the revised main text: [Theoretical models suggest that at more negative potentials, activation

of the Tafel step at adjacent Cu sites promotes preferential *H recombination via the low-barrier HER pathway, thereby suppressing *CHO availability. Furthermore, the DFT calculation results confirm that in the absence of *CHO participation, direct *CO – *CO coupling on Cu(100) (ΔG = 1.04 eV) becomes kinetically and thermodynamically unfavorable relative to HER, resulting in HER dominance at high cathodic potentials on CuO NS.]

6. There are a few minor spelling and typographical errors in the manuscript, Main text, Line 213: The word "indentical" is misspelled and should be corrected to "identical". Main text, Line 491: There is a duplicated word in the phrase "with with experimentally"

Response: We sincerely apologize for these careless typographical errors and are extremely grateful to the reviewer for reading our manuscript so meticulously.

Following your precise corrections, we have changed the misspelled word “indentical” to “identical” (**Page [9], Line [237]**) and removed the duplicated word "with" in the phrase “with experimentally” (**Page [21], Line [541]**).

Furthermore, to ensure the highest quality of presentation, we have conducted a comprehensive and thorough proofreading of the entire revised manuscript and the Supplementary Information to eliminate any other potential spelling, grammatical, or formatting errors.

Reply to Reviewer #3:

This manuscript presents a significant conceptual advance in acidic CO_2 electroreduction by introducing a strategy to regulate proton transfer rather than suppress it. The catalytic performance is outstanding and the integration of molecular and heterogeneous catalysis is highly promising.

However, the structural characterization does not yet fully support the proposed molecular–metal interface and dual-site mechanism. Strengthening the structural evidence would greatly enhance the rigor and impact of the work. I recommend minor revision.

Response: We would like to express our deepest gratitude to the reviewer for the positive evaluation and for explicitly recognizing the significant conceptual advance of our work. We are thrilled that you find our core strategy, regulating the proton transfer pathway rather than simply suppressing it, to be a highly promising integration of molecular and heterogeneous catalysis, and our catalytic performance to be excellent.

We also deeply appreciate your highly constructive and critical feedback regarding the structural characterization. We completely agree with your insightful assessment that strengthening the structural evidence is paramount to fully supporting our proposed molecular–metal interface and the dual-site synergistic mechanism, thereby maximizing the rigor and scientific impact of this manuscript. Guided by your valuable recommendation, we have dedicated significant effort to fortifying the structural evidence in the revised manuscript.

1. The central premise of the manuscript relies on the formation of a well-defined molecular-metal interface, in which TCPP(Co) is anchored to the Cu surface via carboxylate coordination. However, the structural evidence supporting this claim remains largely indirect. The authors rely on FT-IR shifts of $-COO^-$ group, XPS signals (Co 2p and N 1s), and HRTEM observations to support the anchoring of TCPP(Co). While these techniques confirm the presence of the molecular species, they do not provide definitive information regarding the binding configuration

(monodentate or bidentate), the coordination geometry at the Cu surface or the orientation of the porphyrin relative to the catalyst. The authors should explain and show more direct evidence.

Response: We sincerely thank the reviewer for this insightful and constructive comment. We agree that definitive evidence regarding the binding configuration and orientation of the TCPP(Co) molecule is essential to support our central premise of a well-defined molecular-metal interface. To address this, we have conducted additional experimental characterizations, performed comprehensive density functional theory (DFT) calculations, and refined our mechanistic descriptions in the revised manuscript.

Our detailed point-by-point responses and corresponding revisions are as follows:

To provide direct structural evidence and address your concerns regarding the integrity of the anchored TCPP(Co), we have incorporated X-ray absorption spectroscopy (XAS) and spherical aberration-corrected scanning transmission electron microscopy (AC-STEM) characterizations into the revised manuscript. Specifically, in the extended X-ray absorption fine structure (EXAFS) analysis, we utilized Co foil and cobalt phthalocyanine (CoPc) as reference samples. The EXAFS spectra of our TCPP(Co) catalyst distinctly exhibit a dominant Co–N scattering path, closely aligning with the CoPc molecular reference. Crucially, there is a complete absence of the characteristic Co–Co signal, which would otherwise indicate the formation of metallic Co clusters or nanoparticles. This spectral evidence confirms that the Co centers remain atomically dispersed and the precise coordination environment of the porphyrin macrocycle is perfectly preserved during the catalyst preparation (**Fig. R11**).

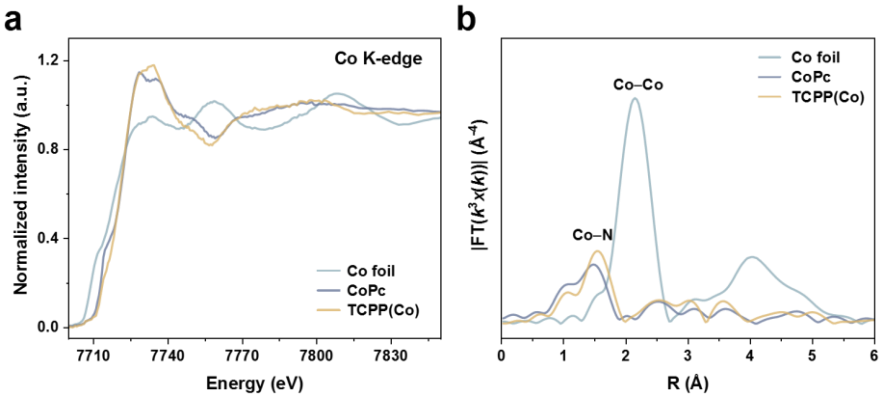

Fig. R11 | a, Normalized Co K-edge XANES spectra and **b,** FT-EXAFS spectra of TCPP(Co), with Co foil and CoPc as references.

Furthermore, this spectroscopic analysis is visually corroborated by our AC-STEM observations. High-angle annular dark-field Scanning transmission electron microscopy (HAADF-STEM) images reveal a uniform distribution of isolated bright spots corresponding to individual Co heavy atoms. There is no observable aggregation or nanocluster formation across the support. Furthermore, the corresponding energy-dispersive X-ray spectroscopy (EDS) elemental mapping acquired in HAADF mode clearly demonstrates the highly uniform and homogenous distribution of Co species throughout the material (**Fig. R12**). Together, the combination of EXAFS and AC-STEM definitively proves the single-atom nature of the TCPP(Co) molecules on the surface, establishing the fundamental structural baseline for the molecular-metal interface discussed in our study.

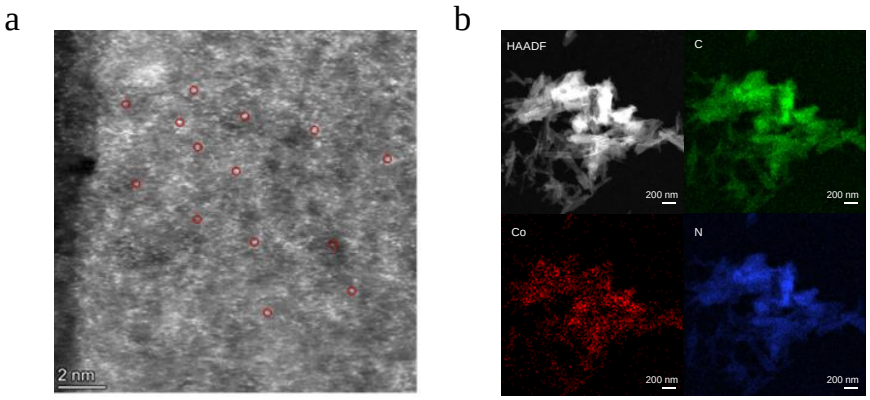

Fig. R12 | a, AC-STEM image (isolated Co atoms are highlighted by red circles) and **b,** HAADF-STEM image with corresponding EDS elemental mapping of TCPP(Co).

High-resolution TEM (HRTEM) allowed us to directly observe the nanoscale molecular layer at the metal-organic interface. Notably, by comparing the catalyst before and after 100 h stability test, we observed that the molecular layer becomes thicker and more pronounced. This structural evolution strongly indicates a dynamic electrochemical self-assembly process, leading to a highly stable bidentate coordination during the reaction (**Fig. R13**).

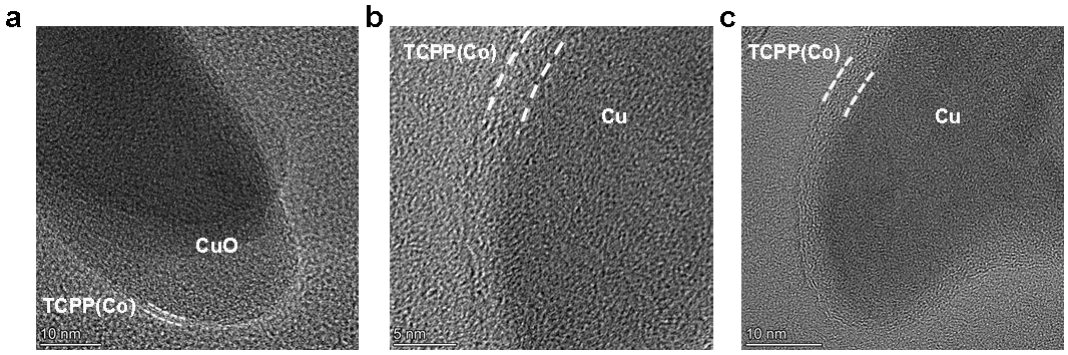

Fig. R13 | HRTEM image of TCo–CuO NS (a) before and (b, c) after 100 h CO_2RR, the thin layer of TCPP(Co) was marked by white line.

To prove the preservation of the single-atom/molecular nature during and after the reaction, we employed a comprehensive suite of orthogonal characterizations, instead of relying on unreliable localized high-magnification mapping, our HAADF-STEM EDS elemental mapping over broader regions clearly demonstrates that the Co species maintain a highly uniform and homogeneous dispersion across the entire catalyst surface (**Supplementary Fig. 19, 20 and Fig. R15**). The complete absence of localized Co enrichment or clustering strongly negates the occurrence of nanoparticle aggregation.

We conducted extensive X-ray photoelectron spectroscopy (XPS) analysis on the samples. The Co 2p spectra show that the chemical state of Co remains completely consistent with its initial molecular coordination environment, with no emergence of zero-valent metallic Co peaks (~778.0 eV) that would signify catalyst degradation or agglomeration (**Fig. R1**).

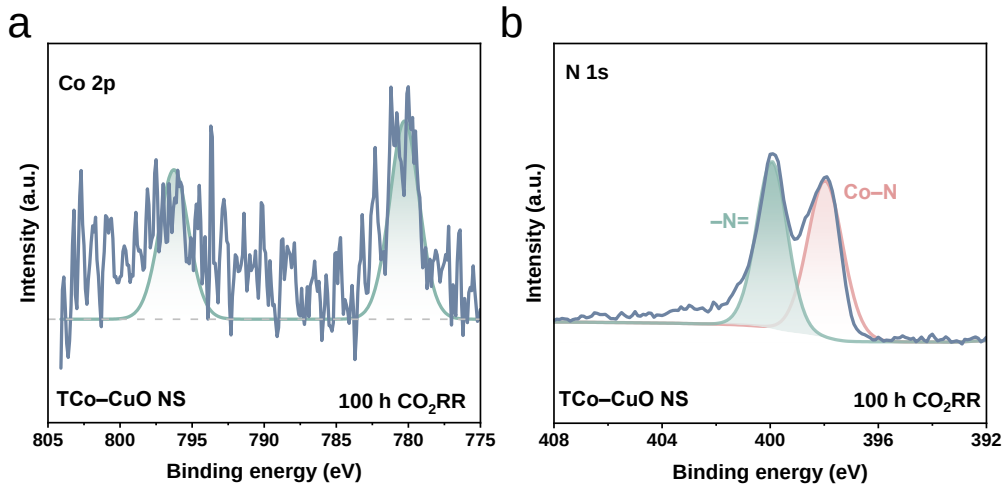

Fig. R1 | High-resolution XPS spectra of the catalyst after 100 h stability test at 0.2 A cm^{-2}, **a,** Co 2p and **b,** N 1s.

To explicitly address the binding configuration (monodentate vs. bidentate), we conducted a detailed comparative analysis of the attenuated total reflection Fourier transform infrared spectroscopy (ATR-FTIR) spectra before and after 100 h stability test. By analyzing the wavenumber difference between the asymmetric and symmetric stretching vibrations of the $–COO^-$ groups, we obtained definitive spectroscopic evidence. The specific Δv values confirm the orientation of the TCPP(Co) molecules and prove the transition to a stable bidentate coordination mode post-reaction (***Coordination Chemistry Reviews*****,** 1980, 33, 3, 227-250) (**Fig. R9**).

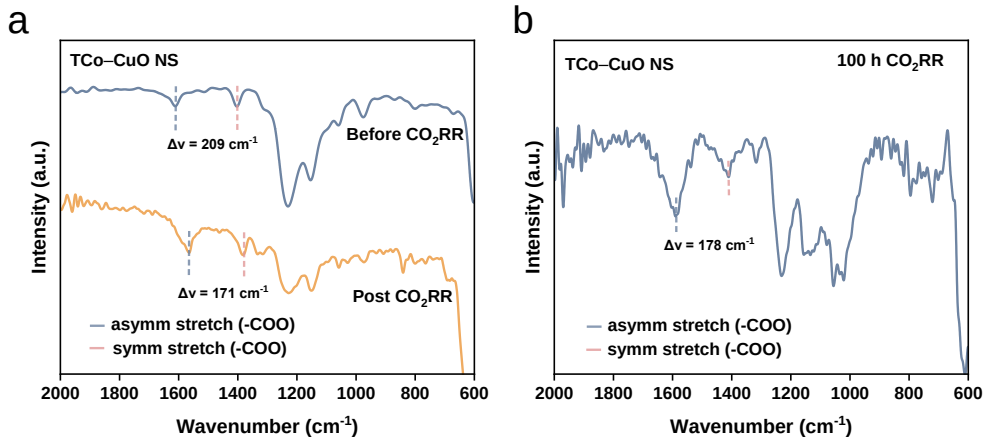

Fig. R9 | ATR-FTIR spectra of TCo–CuO NS **a,** before, after 3 h CO_2RR test and **b,** after 100 h CO_2RR test at 0.2 A cm^{-2}.

Then, we have performed systematic DFT calculations to directly compare the energetics of monodentate versus bidentate coordination, using both the simplified BZA model and the full TCPP(Co) complex. These results provide direct computational evidence supporting the bidentate anchoring configuration employed throughout our study. To determine the most favorable binding mode of the carboxylate anchor on the Cu surface, we calculated the adsorption energies of benzoic acid (BZA) on Cu(100) in both monodentate and bidentate configurations. The bidentate configuration was found to be more stable by approximately 0.80 eV compared to the monodentate upright adsorption mode. This significant energy difference indicates that the bidentate coordination is thermodynamically preferred. Moreover, in the monodentate upright configuration, the phenyl ring is oriented away from the surface, missing the additional stabilization from van der Waals interactions between the aromatic ring and the Cu substrate, which further disfavors this binding mode under realistic conditions. To confirm that this bidentate preference persists in the full molecular system, we performed full structural optimization of the complete TCPP(Co) complex adsorbed on a 10 × 10 Cu(100) supercell (total 485 atoms). Crucially, the energetic analysis reveals that the bidentate coordination of the complete TCPP(Co) complex is thermodynamically more stable than the monodentate configuration by 0.35 eV. In the optimized structure, both carboxylate groups of the TCPP(Co) molecule adopt a clear bidentate coordination mode on the Cu surface (**Fig. R14**). This result directly demonstrates that the bidentate configuration is not merely a simplification introduced by the BZA model, but rather the intrinsic binding motif of the TCPP(Co) modifier on Cu under the investigated conditions. The consistency in binding mode between the simplified BZA model and the full TCPP(Co) complex validates our tiered modeling strategy. The bidentate coordination observed in both systems ensures that the local electronic structure at the –COO–Cu interface is faithfully reproduced in the BZA model, justifying its use for the thermodynamic analysis of the C–C coupling steps.

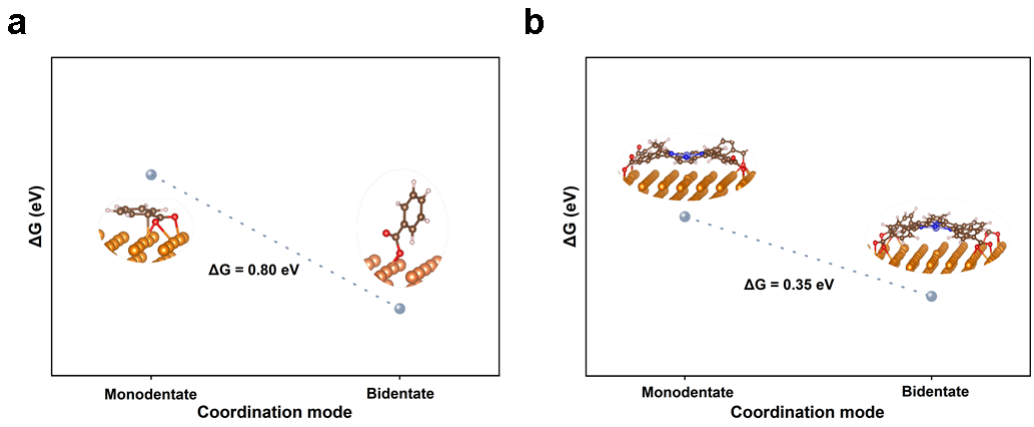

Fig. R14 | Calculated relative free energy (ΔG) profiles comparing the monodentate and bidentate configurations for (a) the simplified benzoic acid (BZA) model and (b) the complete TCPP(Co) complex . The bidentate coordination is thermodynamically preferred in both systems.

Based on your feedback and our newly acquired evidence, we have corrected our initial description of the pre-electroreduction state. Instead of claiming a definitive monodentate coordination prior to the reaction, we now accurately infer that TCPP(Co) initially adsorbs onto the CuO(200) surface via van der Waals forces or weak monodentate coordination (***J. Am. Chem. Soc.*** *2026,* 148, 13444-13453). During the electroreduction process, this dynamically evolves into a highly stable bidentate coordination on the newly reduced Cu surface. Crucially, we would like to emphasize that our density functional theory (DFT) calculations were strictly modeled upon the actual in operando catalytic state during the electroreduction process, namely, TCPP(Co) anchored to the newly reduced Cu(100) surface via the highly stable bidentate coordination. Therefore, refining the description of the initial pre-electroreduction state does not alter the structural models utilized in our theoretical simulations. Consequently, the validity of our computational results and the derived mechanistic conclusions remain entirely unaffected by this clarification.
The newly added text is as follows,

Corresponding revision:

❑ The modification has been highlighted in **Page [9], Line [231]** of the revised main text: [Furthermore, extended X-ray absorption fine structure (EXAFS)

analysis reveals a dominant Co–N path without any Co–Co scattering signals, confirming the strict atomic dispersion of the Co centers. This single-atom nature is visually corroborated by aberration-corrected STEM (AC-STEM) and elemental mapping, which demonstrate a highly uniform distribution of isolated Co atoms across the support without any metallic aggregation (**Supplementary Fig. 16a-16d**).]

❑ The modification has been highlighted in **Page [9], Line [238]** of the revised main text: [HRTEM analysis further indicates that TCPP(Co) molecules are initially anchored on the predominant CuO(200) facet via van der Waals forces or weak monodentate coordination prior to CO_2RR (**Supplementary Fig. 17a**), with the molecular overlayer clearly distinguishable (**Supplementary Fig. 17b**).]

❑ The modification has been highlighted in **Page [8], Line [212]** of the revised main text: [During the synthesis of TCPP(M)–CuO, TCPP(M) initially adsorbs onto the CuO NS surface via van der Waals interactions or weak monodentate coordination between the terminal carboxyl groups (–COO-) and Cu^{2+} within the lattice.]

❑ The modification has been highlighted in **Page [9], Line [246]** of the revised main text: [which is computationally verified to be thermodynamically more stable than the monodentate mode by 0.346 eV (**Supplementary Fig. 19**).]

❑ To provide a more cohesive presentation of these results, we have integrated **Fig. R11** and **Fig. R12** into a single figure. This new figure has been added to the revised Supplementary Information as **Supplementary Figure 16**.

❑ To provide a more cohesive presentation of these results, we have integrated **Fig. R9** and **Fig. R14** into a single figure. This new figure has been added to the revised Supplementary Information as **Supplementary Figure 18**.

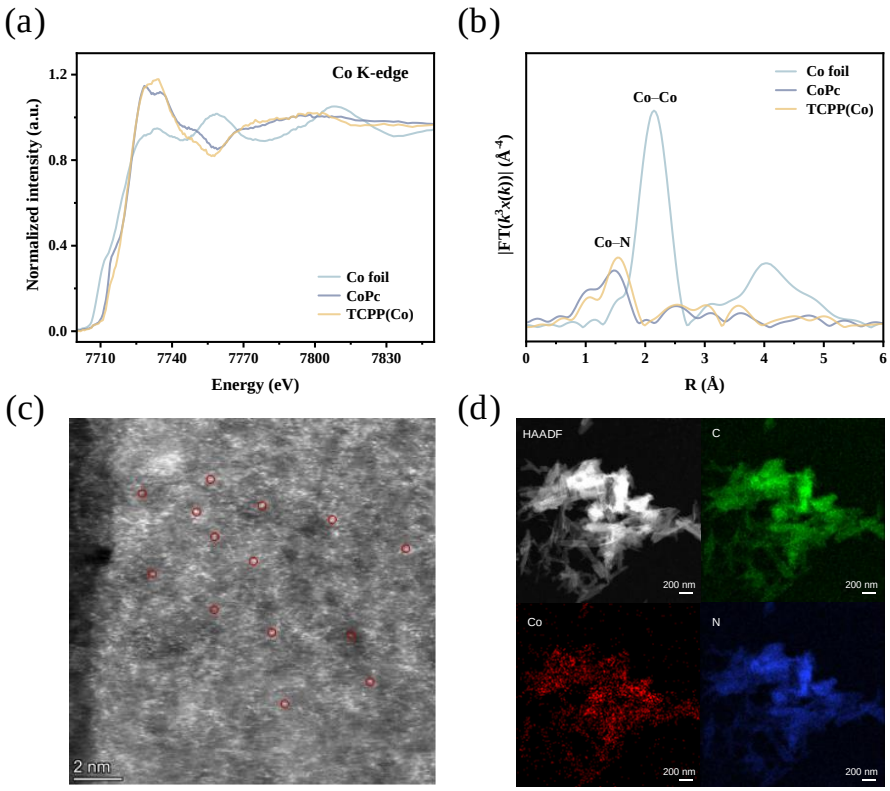

Supplementary Figure 16. (a) Normalized Co K-edge XANES spectra, (b) FT-EXAFS spectra of TCPP(Co), with Co foil and cobalt phthalocyanine (CoPc) as references. (c) AC-STEM image (isolated Co atoms are highlighted by red circles), (d) HAADF-STEM image and the corresponding EDS elemental mapping of TCPP(Co).

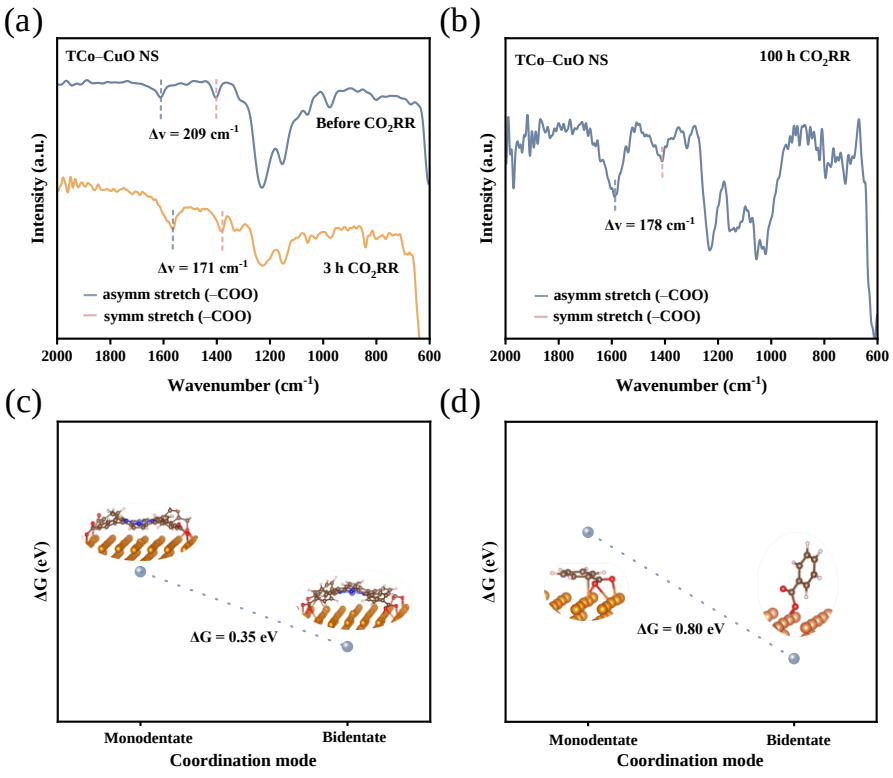

Supplementary Figure 18. ATR-FTIR spectra of TCo-CuO NS (a) before and after 3 h CO_2RR test, (b) after 100 h CO_2RR test at 0.2 A cm^{-2}. Calculated relative free energy (ΔG) profiles comparing the monodentate and bidentate configurations for (c) the simplified benzoic acid (BZA) model and (d) the complete TCPP(Co) complex. The bidentate coordination is thermodynamically preferred in both systems.

2. The manuscript claims uniform dispersion of TCPP(Co) based on EDS mapping; however, this technique lacks sufficient spatial resolution to assess molecular-scale distribution. Moreover, the manuscript does not provide quantitative information on the loading amount of TCPP(Co), surface coverage, or the density of active sites. This information is essential for understanding structure-activity relationships and for normalizing catalytic activity.

Response: We sincerely thank the reviewer for this highly insightful and constructive comment. We completely agree that low-resolution EDS is insufficient to confirm molecular-scale distribution, and that precise quantitative data on loading amounts and active site density are strictly required for establishing reliable structure-activity relationships. To comprehensively address these concerns, we have conducted a series of multi-scale structural characterizations and systematic quantitative analyses in the revised manuscript.

Ultimately, to confirm the fundamental structural nature of the active centers, we employed AC-STEM and EXAFS. The AC-STEM images reveal isolated bright spots corresponding to individual Co heavy atoms, while the EXAFS analysis confirms a dominant Co–N scattering path with a complete absence of Co–Co metallic clustering (**Fig. R11** and **R12**). Together, these techniques unequivocally demonstrate the single-atom, molecular-scale dispersion of TCPP(Co) on the catalyst surface.

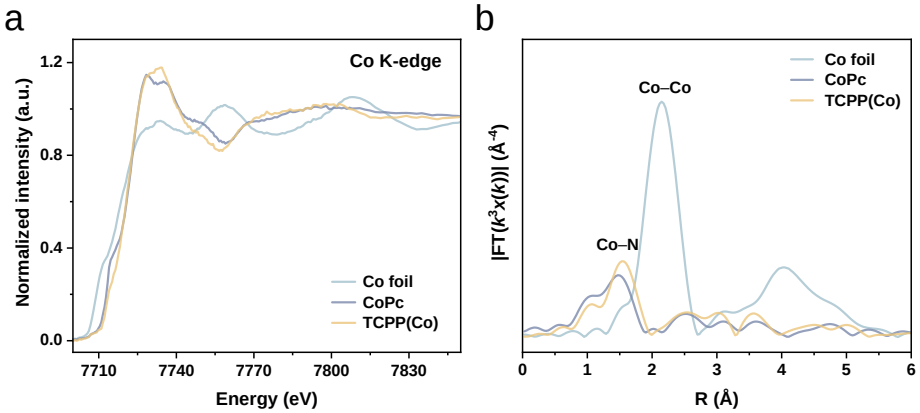

Fig. R11 | a, Normalized Co K-edge XANES spectra and **b,** FT-EXAFS spectra of TCPP(Co), with Co foil and CoPc as references.

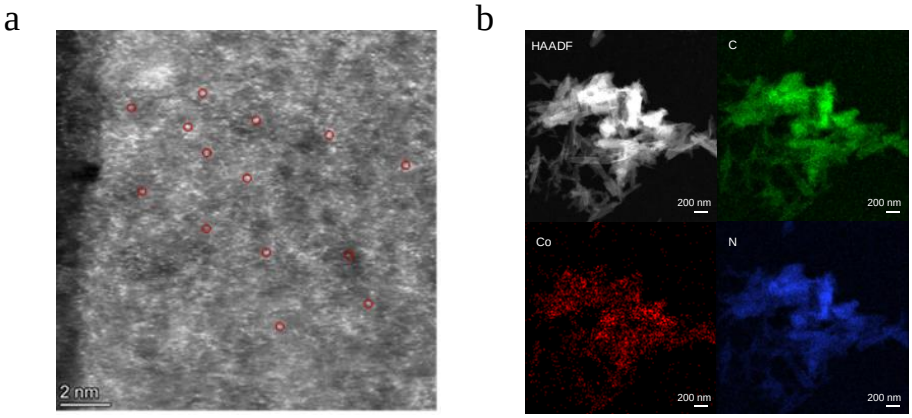

Fig. R12 | a, AC-STEM image (isolated Co atoms are highlighted by red circles) and **b,** HAADF-STEM image with corresponding EDS elemental mapping of TCPP(Co).

To provide direct evidence of the molecular-scale and atomic-scale distribution of the TCPP(Co) modifier, we have upgraded our electron microscopy and spectroscopic characterizations across multiple length scales. First, we performed HAADF-STEM and corresponding EDS elemental mapping at a 50 nm scale, which clearly illustrates the highly uniform dispersion of Co, N, and Cu elements (**Fig. R15**). In addition, the HAADF-STEM images reveal a distinct overlayer enveloping the catalyst surface. This visible coating serves as corroborating evidence for the presence of the molecular TCPP(Co) layer.

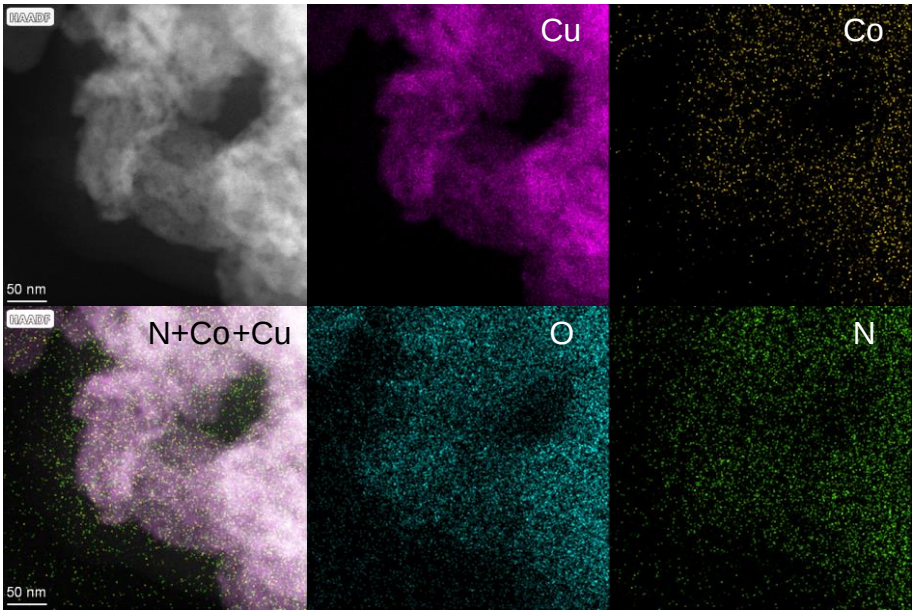

Fig. R15 | HAADF-STEM image and corresponding EDS elemental mapping of TCo–CuO NS after 100 h stability test at 0.2 A cm^{-2} at 50 nm scale.

Proceeding to the molecular scale, HRTEM was utilized to directly visualize the intact, amorphous molecular overlayer uniformly coated on the highly crystalline CuO surface before and after 100 h CO_2RR test (**Fig. R13**).

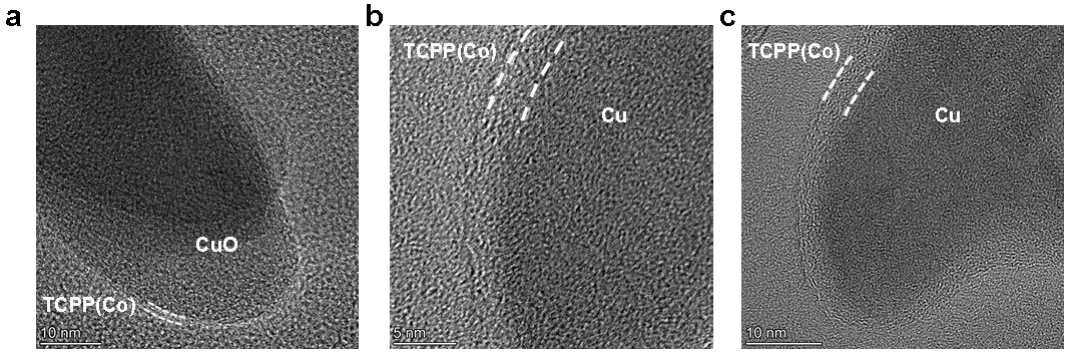

Fig. R13 | HRTEM image of TCo–CuO NS (a) before and (b, c) after 100 h CO_2RR test, the thin layer of TCPP(Co) was marked by white line.

Furthermore, to address the request for precise quantitative information, we systematically investigated both the bulk loading amount and the surface coverage using inductively coupled plasma optical emission spectrometry (ICP-OES) and XPS. Calculated from the initial precursor feed, the theoretical Co/Cu atomic ratio for the optimally loaded sample (1×) is approximately 0.94%. However, ICP-OES

measurements reveal that the actual bulk Co/Cu atomic ratio for this optimal sample is 0.50% (Cu:Co = 199:1). This deviation is highly reasonable, as the thorough washing processes effectively remove weakly physisorbed molecules, leaving only the robustly chemisorbed active species. Interestingly, when the precursor feed is tripled for the excessively coated sample (3×), the actual bulk Co/Cu ratio only slightly increases to 0.64% (Cu:Co = 157:1). This minimal increase indicates that the available chemical anchoring sites on the CuO surface approach saturation, forcing the excessive TCPP(Co) to physically pile up at the interface (**Table R2**). Additionally, post-reaction XPS analysis of the optimal sample after 100 h of continuous electrolysis shows that the surface Co ratio merely changes from 3.37% to 2.75%, providing robust quantitative proof of the exceptional long-term stability of the molecular coverage (**Table R3**).

The electrochemically active surface area (ECSA) was determined by $A_{ECSA}=C_{dl}/C_s$, where C_s is 28.2 mF cm^{-2} (**Supplementary Table 6**) and C_s is assumed to be 0.020 mF cm^{-2} for Cu-based surfaces (***Pure and Applied Chemistry***, 1991, 63(5), 711-734), yielding a roughness factor of 1410. Given the catalyst loading of 1 mg cm^{-2} and the ICP-determined Cu:Co atomic ratio of 199:1, the molar amount of Co per geometric cm^2 is calculated by combining the bulk CuO mass and the precise atomic ratio:

$$\frac{1\times10^{-3}\ g/79.55\ g\ mol^{-1}}{199}=6.317\times10^{-8}\ mol$$

The active site density is obtained by dividing the Co molar amount by the ECSA to reflect the intrinsic density of Co sites dispersed over the nano-rough surface:

$$\frac{6.317\times10^{-8}\ mol}{1410\ cm^{-2}}=4.48\times10^{-11}\ mol\ cm^{-2}$$

The molar density of $4.48\times10^{-11}\ mol\ cm^{-2}$ is converted to the absolute number of sites per square nanometer by multiplying by the Avogadro constant ($N_A = 6.022\times10^{23}\ mol^{-1}$) and converting the area unit from cm^2 to nm^2 ($1\ cm^2 = 10^{14}\ nm^2$), which yields approximately 0.27 sites nm^{-2}.

This density corresponds to 0.27 sites nm^{-2}. Based on the optimized geometric configuration obtained from our rigorous DFT modeling, the exact projected area of

the anchored TCPP(Co) molecule is determined to be 1.73 nm^2, the TCPP(Co) surface coverage is:

$$0.27\ site\ nm^{-2} \times 1.73\ nm^2/site = 46.71\%$$

Table R2 | Actual bulk Co/Cu atomic ratios of the optimal (1×) and excessively loaded (3×) TCo–CuO NS catalysts determined by ICP-OES.

Samples	Theoretical Co/Cu atomic ratio	Co/Cu atomic ratio
TCo–CuO NS	0.94%	0.50%
TCo–CuO NS-3	2.82%	0.64%

Table R3 | Detailed fitting position of TCo–CuO NS and TCo–CuO NS (Post CO_2RR) based on high-resolution XPS spectra.

Catalysts	Cu 2p Fitting position (eV)	Co 2p Fitting position (eV)	Atomic ratio Cu:Co
TCo–CuO NS	934.70/954.51	780.42/795.35	96.63:3.37
TCo–CuO NS (Post CO_2RR)	934.45/954.38	780.47/795.42	97.25:2.75
TCo–CuO NS-3	934.58/954.35	779.75/794.72	96.01:3.99

Corresponding revision:

❑ The modification has been highlighted in **Page [10], Line [249]** of the revised main text: [The uniform distribution of TCPP(Co) on the CuO NS is evident prior to the reaction (**Supplementary Fig. 19)** and is maintained after CO_2RR, as confirmed by energy-dispersive X-ray spectroscopy (EDS) elemental mapping (**Supplementary Fig. 20**). Moreover, post-stability test analyses demonstrate the robust nature of the catalyst. XPS spectra verify the sustained presence of the Co centers, HAADF-STEM EDS elemental mapping confirms the persistent uniform dispersion of the Co species

after 100 h of continuous operation (**Supplementary Fig. 21**), and HRTEM images reveal the intact amorphous molecular overlayer, confirming the preservation of the molecular-metal interface during prolonged electrolysis (**Supplementary Fig. 22**)]

❑ The modification has been highlighted in **Page [10], Line [264]** of the revised main text: [To determine the precise absolute loading, inductively coupled plasma optical emission spectrometry (ICP-OES) was performed, revealing an actual bulk Co/Cu atomic ratio of 0.50% (**Supplementary Table 2**). Crucially, semi-quantitative XPS analysis reveals a surface Co proportion of 3.37%, significantly exceeding the theoretical bulk ratio (~0.94%), which directly confirms the successful surface enrichment and molecular anchoring of TCPP(Co) (**Supplementary Table 3**).]

❑ The information presented in **Fig. R15** has been used as **Supplementary Figure 21** in the revised Supplementary Information.

❑ We have incorporated all these quantitative ICP and XPS results into **Supplementary Table 2 and 3** of the revised Supplementary Information.

3. Structural stability of the molecular layer after long-term electrolysis should be more thoroughly characterized.

Response: We thank the reviewer for this insightful comment. We fully agree that the structural stability of the molecular overlayer after prolonged electrolysis is crucial for validating both the catalyst design and the proposed mechanistic interpretation. In response, we have carried out additional post-electrolysis characterizations after 100 h stability test at 0.2 A cm^{-2}, including ATR-FTIR, XPS, and HRTEM, and we have also performed a supplementary ICP leaching analysis to evaluate the stability of the Co center in the electrolyte phase.

The post-reaction ATR-FTIR spectrum still displays clear carboxylate-related vibrational features, indicating that the anchoring groups of the molecular layer remain on the electrode after long-term electrolysis. Moreover, the peak separation between the asymmetric and symmetric carboxylate stretching modes is consistent

with the preservation of bidentate carboxylate coordination, supporting the structural robustness of the anchoring interaction between TCPP(Co) and the Cu surface (**Fig. R9**).

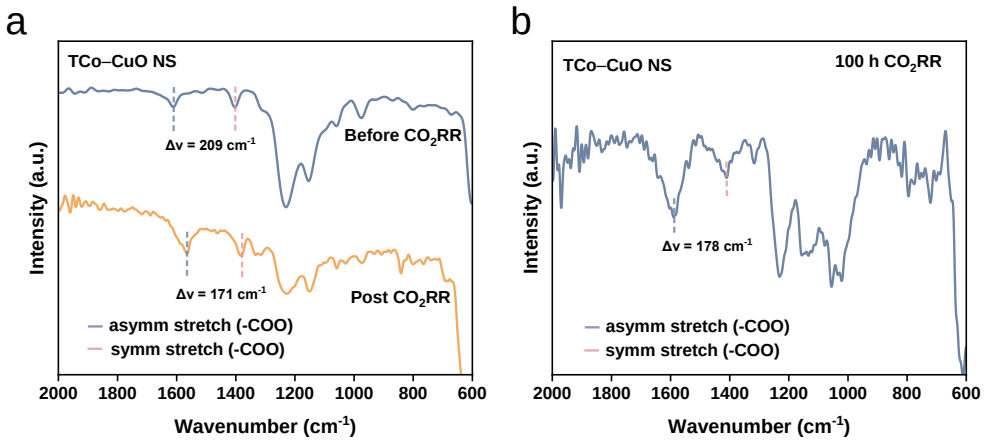

Fig. R9 | ATR-FTIR spectra of TCo–CuO NS **a,** before, after 3 h CO_2RR test and **b,** after 100 h CO_2RR test at 0.2 A cm^{-2}.

The post-reaction XPS spectra further shows that the characteristic Co-related signals remain clearly detectable after 100 h electrolysis, indicating that the Co center is retained during prolonged operation and does not undergo obvious loss (**Fig. R1** and **Table R3**). This result is important because it confirms that the molecularly defined active unit remains present under catalytic conditions.

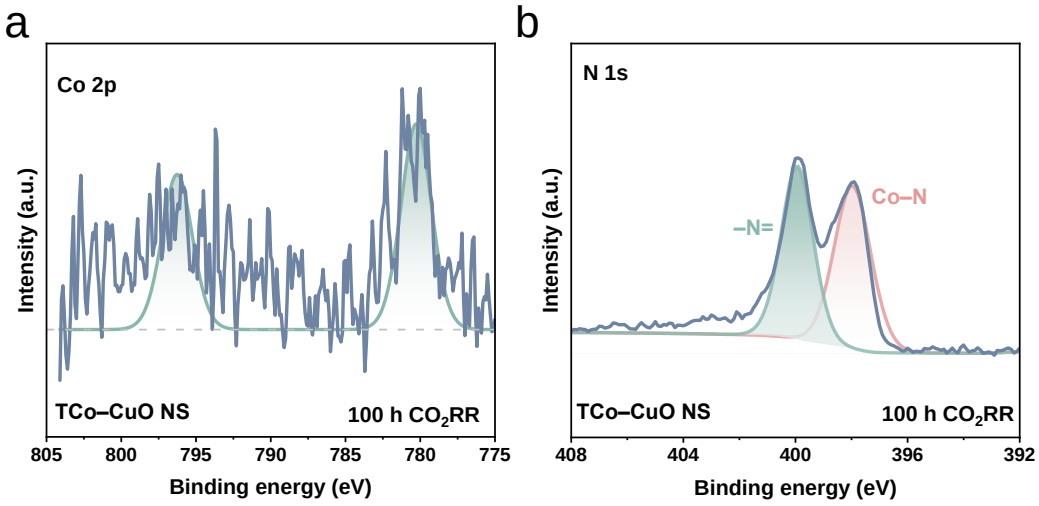

Fig. R1 | High-resolution XPS spectra of the catalyst after 100 h stability test at 0.2 A cm^{-2}, **a,** Co

2p and **b,** N 1s.

To obtain direct microscopic evidence, we further ultrasonically detached the catalyst particles from the electrode after 100 h CO_2RR test and examined them by HRTEM. The HRTEM images clearly reveal the continued presence of the amorphous molecular overlayer, directly demonstrating that the molecular layer remains on the catalyst surface after long-term electrolysis.

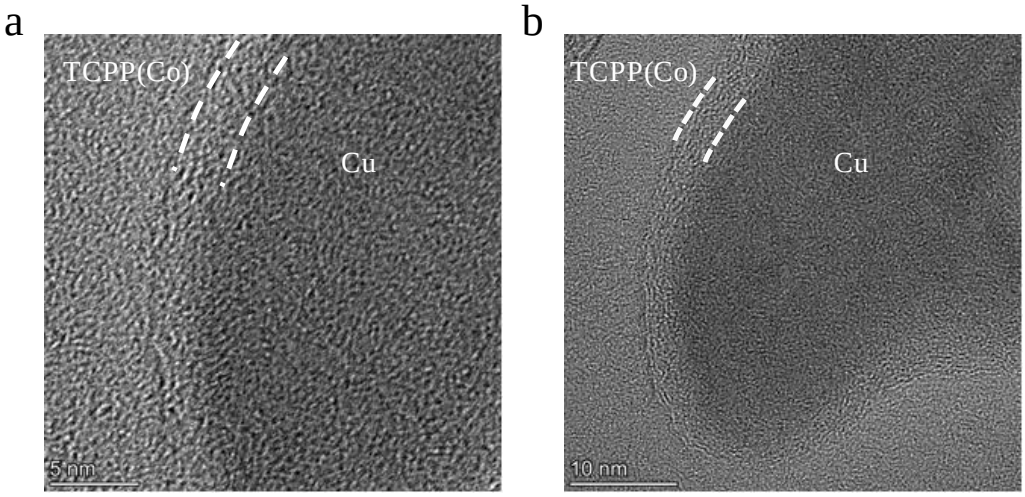

Fig. R8 | HRTEM image of TCo–CuO NS after 100 h CO_2RR test, the thin layer of TCPP(Co) was marked by white line.

Taken together, these additional data provide complementary spectroscopic, microscopic, and solution-phase evidence that the TCPP(Co) molecular layer remains stably anchored during long-term electrolysis, with both the bidentate carboxylate coordination and the Co center being preserved, while the amorphous molecular overlayer remains directly observable after reaction. The corresponding results and discussion have now been added to the revised manuscript and Supporting Information.

Corresponding revision:

❑ The modification has been highlighted in **Page [10], Line [249]** of the revised main text: [The uniform distribution of TCPP(Co) on the CuO NS is evident prior to

the reaction (**Supplementary Fig. 19)** and is maintained after CO_2RR, as confirmed by energy-dispersive X-ray spectroscopy (EDS) elemental mapping (**Supplementary Fig. 20**). Moreover, post-stability test analyses demonstrate the robust nature of the catalyst. High-angle annular dark-field scanning transmission electron microscopy (HAADF-STEM) EDS elemental mapping confirms the persistent uniform dispersion of the Co species after 100 h of continuous operation (**Supplementary Fig. 21**). XPS spectra verify the sustained presence of the Co centers (**Supplementary Fig. 22a-22b and Supplementary Note 2**), and HRTEM images reveal the intact amorphous molecular overlayer, confirming the preservation of the molecular-metal interface during prolonged electrolysis (**Supplementary Fig. 22c-22d and Supplementary Note 3**]

❑ The modification has been highlighted in **Page [9], Line [243]** of the revised main text: [The separation between asymmetric and symmetric $–COO^-$ stretching modes ($\Delta\nu$) decreases from 209 cm^{-1} to 171/178 cm^{-1}, indicative of a dynamic structural evolution into a highly stable bidentate coordination between in situ-generated metallic Cu and TCPP(Co), which is computationally verified to be thermodynamically more stable than the monodentate mode by 0.35 eV (**Supplementary Fig. 18c and 18d**).]

❑ To provide a more cohesive presentation of these results, we have integrated **Fig. R1** and **Fig. R8** into a single figure. This new figure has been added to the revised Supplementary Information as **Supplementary Figure 22**.

❑ To provide a more cohesive presentation of these results, we have integrated **Fig. R9** and **Fig. R14** into a single figure. This new figure has been added to the revised Supplementary Information as **Supplementary Figure 18**.

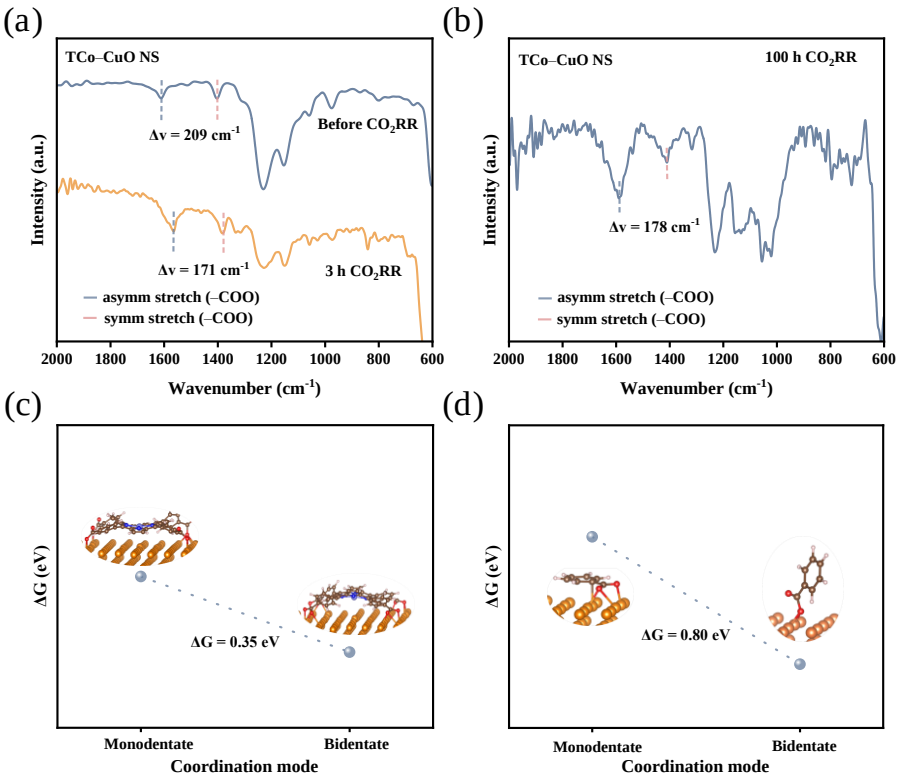

Supplementary Figure 18. ATR-FTIR spectra of TCo-CuO NS (a) before and after 3 h CO_2RR, (b) after 100 h CO_2RR test at 0.2 A cm^{-2}. Calculated relative free energy (ΔG) profiles comparing the monodentate and bidentate configurations for (c) the simplified benzoic acid (BZA) model and (d) the complete TCPP(Co) complex. The bidentate coordination is thermodynamically preferred in both systems.

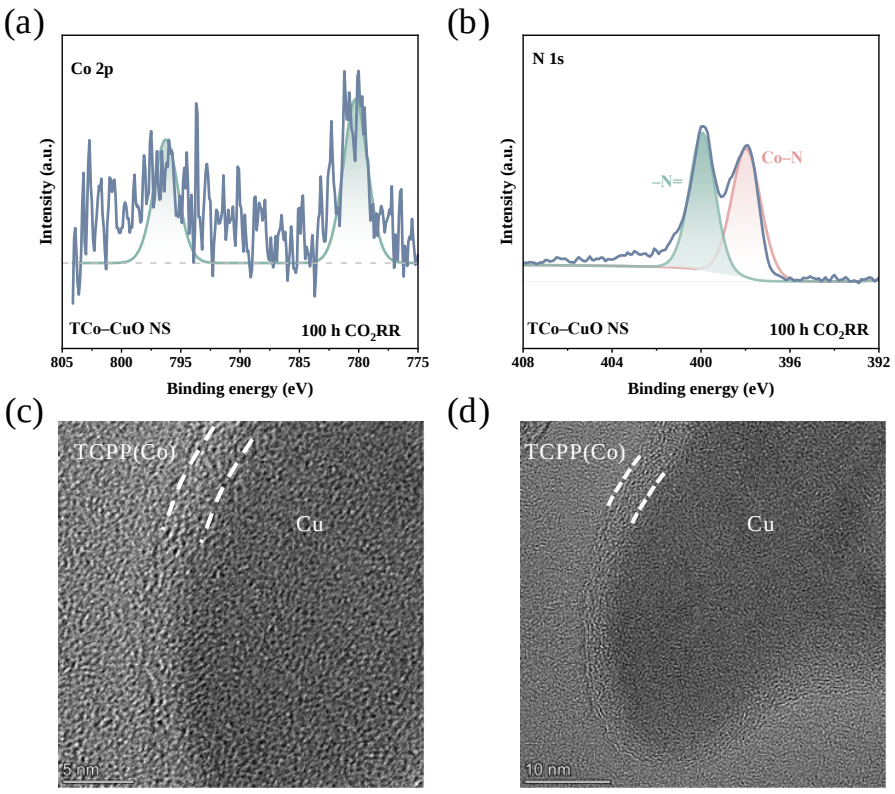

Supplementary Figure 22. High-resolution XPS spectra of TCo-CuO NS (a) Co 2p and (b) N 1s. (c, d) HRTEM image of TCo-CuO NS, the thin layer of TCPP(Co) was marked by white line, after 100 h stability test at 0.2 A cm^{-2}.

Supplementary Note 2: We acquired the Co 2p and N 1s high-resolution XPS spectra of the post-100 h sample (**Supplementary Figure 22a-22b**). These spectra perfectly match those of the pristine catalyst, with no emergence of zero-valent Co or CoO species, confirming that the Co–N_4 coordination centers remain highly stable under prolonged cathodic polarization.

Supplementary Note 3: To provide even more comprehensive proof, we also supplemented post-100 h HRTEM image, which shows the preserved nanoscale molecular layer (**Supplementary Figure 22c-22d**). Along with an accelerated continuous ICP leaching test to further corroborate the excellent anchoring stability of TCPP(Co).